ARRHYTHMIAS

An improved reporter identifies ruxolitinib as a potent and cardioprotective CaMKII inhibitor

Oscar E. Reyes Gaido[1]†, Nikoleta Pavlaki[2]†, Jonathan M. Granger[1], Olurotimi O. Mesubi[1], Bian Liu[3], Brian L. Lin[1], Alan Long[4], David Walker[2], Joshua Mayourian[2], Kate L. Schole[1], Chantelle E. Terrillion[5], Lubika J. Nkashama[1], Mohit M. Hulsurkar[6], Lauren E. Dorn[6], Kimberly M. Ferrero[1], Richard L. Huganir[3], Frank U. Müller[7], Xander H. T. Wehrens[6,8], Jun O. Liu[4], Elizabeth D. Luczak[1], Vassilios J. Bezzerides[2]*, Mark E. Anderson[1,9]*

Ca^{2+}/calmodulin-dependent protein kinase II (CaMKII) hyperactivity causes cardiac arrhythmias, a major source of morbidity and mortality worldwide. Despite proven benefits of CaMKII inhibition in numerous preclinical models of heart disease, translation of CaMKII antagonists into humans has been stymied by low potency, toxicity, and an enduring concern for adverse effects on cognition due to an established role of CaMKII in learning and memory. To address these challenges, we asked whether any clinically approved drugs, developed for other purposes, were potent CaMKII inhibitors. For this, we engineered an improved fluorescent reporter, CaMKAR (CaMKII activity reporter), which features superior sensitivity, kinetics, and tractability for high-throughput screening. Using this tool, we carried out a drug repurposing screen (4475 compounds in clinical use) in human cells expressing constitutively active CaMKII. This yielded five previously unrecognized CaMKII inhibitors with clinically relevant potency: ruxolitinib, baricitinib, silmitasertib, crenolanib, and abemaciclib. We found that ruxolitinib, an orally bioavailable and U.S. Food and Drug Administration–approved medication, inhibited CaMKII in cultured cardiomyocytes and in mice. Ruxolitinib abolished arrhythmogenesis in mouse and patient-derived models of CaMKII-driven arrhythmias. A 10-min pretreatment in vivo was sufficient to prevent catecholaminergic polymorphic ventricular tachycardia, a congenital source of pediatric cardiac arrest, and rescue atrial fibrillation, the most common clinical arrhythmia. At cardioprotective doses, ruxolitinib-treated mice did not show any adverse effects in established cognitive assays. Our results support further clinical investigation of ruxolitinib as a potential treatment for cardiac indications.

INTRODUCTION

Cardiovascular disease is a leading cause of premature death, with more than half a billion patients affected worldwide (*1*). The multifunctional Ca^{2+}/calmodulin-dependent protein kinase II (CaMKII) contributes to physiological regulation of Ca^{2+} cycling in cardiomyocytes (CMs) but is unexpectedly dispensable for cardiac function (*2*–*4*). In contrast, excessive CaMKII activity is cardiotoxic, and CaMKII inhibition is protective in numerous models of inherited and acquired heart diseases and arrhythmias (*5*–*13*). CaMKII hyperactivity is, in part, a consequence of catecholamine stimulation, but clinically approved drugs that inhibit β-adrenergic receptors ("β blockers") are ineffective at preventing increased CaMKII activity in myocardia obtained from patients with heart failure (*14*). Thus, developing safe and effective molecules to directly inhibit CaMKII activity is a major unmet need.

Although several inhibitory modalities have been described, none have reached the clinic because of various limitations. KN-62 and KN-93 were the first CaMKII inhibitors (*15*, *16*). These allosteric inhibitors alleviate CaMKII toxicity in animal models (*7*, *11*, *17*). Although these compounds remain popular as experimental tools, they were clinically hampered by low potency [median inhibitory concentration (IC_{50}) > 2 μM], prohibitive off-target toxicities, and failure to inhibit autonomously hyperactive CaMKII (*18*–*20*). KN-93 has been recently shown to be a calmodulin inhibitor, which explains its inability to inhibit active CaMKII (*21*). CaMKII inhibitory peptides (such as CaMKII-IN and autocamtide-2–related inhibitory peptide) have served as powerful genetic tools with impressive affinity and specificity (*22*, *23*) but have failed to translate because of the challenges of peptide delivery: short plasma half-life, cell impermeability, and suboptimal viral delivery to human myocardium (*24*). Although peptides can be modified to enhance cell penetrance and have reached clinical trials for other indications, these modifications have not yielded clinically viable CaMKII inhibition. To address these limitations, several adenosine triphosphate (ATP)–competitor small molecules have been identified or developed (*25*–*29*). From these, only the natural derivative 3′,4′-dihydroxyflavonol (DiOHF) has made it to a human trial (*30*); this study intended to inhibit CaMKII after ischemia/reperfusion injury but yielded negative results, which were thought to be due to low potency against CaMKII (*31*). Because

[1]Department of Medicine, Johns Hopkins University School of Medicine, Baltimore, MD 21205, USA. [2]Department of Cardiology, Boston Children's Hospital and Harvard Medical School, Boston, MA 02115, USA. [3]Solomon H. Snyder Department of Neuroscience, Johns Hopkins School of Medicine, Baltimore, MD 21205, USA. [4]Department of Pharmacology and Molecular Sciences, Johns Hopkins University School of Medicine, Baltimore, MD 21205, USA. [5]Department of Psychiatry and Behavioral Sciences, Johns Hopkins University School of Medicine, Baltimore, MD 21205, USA. [6]Cardiovascular Research Institute and Department of Integrative Physiology, Baylor College of Medicine, Houston, TX 77030, USA. [7]Institute of Pharmacology and Toxicology, University of Münster, Münster 48149, Germany. [8]Departments of Medicine, Neuroscience, and Pediatrics, Center for Space Medicine, Baylor College of Medicine, Houston, TX 77030, USA. [9]Division of Biological Sciences and the Pritzker School of Medicine, University of Chicago, Chicago, IL 60637, USA.
*Corresponding author. Email: vassilios.bezzerides@cardio.chboston.org (V.J.B.); andersonm1@bsd.uchicago.edu (M.E.A.)
†These authors contributed equally to this work.

CaMKII is important for long-term potentiation and is abundant in excitatory synapses (*32*), concern for adverse effects on learning and memory has been a major obstacle to developing CaMKII inhibitors (*24*). We reasoned that discovery of an approved medication, preferably in broad use, with potent CaMKII inhibitory properties would provide critical insights to inform translational researchers, patients, and industry about the viability of CaMKII inhibitors for clinical use.

Development of small-molecule inhibitors could be facilitated by a reporter with high-throughput capability, but existing CaMKII reporters are not suitable for this. A seminal reporter, Camui, suffers from low dynamic range and reports on conformational changes rather than enzymatic activity (*33*, *34*). A more recent reporter, fluorescence resonance energy transfer–based sensor for CaMKII activity (FRESCA), elegantly bypassed this obstacle by sensing CaMKII activity via direct substrate phosphorylation of the reporter (*35*). This improvement over Camui is limited by FRESCA's dynamic range, which is even lower than that of Camui (~2.7%). On the basis of these limitations, we sought to develop a CaMKII activity reporter that features both high sensitivity and direct kinase sensing, unlike FRESCA or Camui, which have only one of these qualities, thereby making it tractable for in cellulo screening.

In the present study, we address the two major gaps outlined above. First, we engineered a genetically encoded CaMKII activity reporter for live cell screening featuring the highest sensitivity and kinetics reported for a CaMKII reporter. Then, we screened 4475 compounds that have reached human trials and/or U.S. Food and Drug Administration (FDA) approval and identified several compounds capable of inhibiting hyperactive CaMKII. From these, ruxolitinib displayed outstanding repurposing characteristics, including high potency at relevant concentrations, low toxicity, and known low brain penetrance. Ruxolitinib prevented inherited and acquired arrhythmias arising from CaMKII hyperactivity, including catecholaminergic polymorphic ventricular tachycardia (CPVT) and atrial fibrillation (AF), in validated murine disease models without impairing cognitive function.

RESULTS

Development of a CaMKII reporter suitable for high-throughput screening

The discovery of circularly permuted green fluorescent protein (cpGFP) has led to numerous reporters that detect ions, metabolites, and enzyme activity by coupling reconstitution of GFP fluorescence with the process of interest (*36*–*38*). Using kinase-sensing cpGFP (*38*), we engineered a new CaMKII activity reporter. Screening among known CaMKII substrates, the CaMKII autophosphorylation peptide MHRQETVDCLK (autoregulatory domain sequence shared by CaMKIIα/δ) fused to the 5′ end of kinase-sensing cpGFP led to the highest CaMKII-dependent response (fig. S1A). We refer to this reporter as CaMKAR (CaMKII activity reporter), composed of the substrate peptide, cpGFP, and a phosphorylated amino acid binding domain. Upon phosphorylation of the substrate by CaMKII, the phosphoresidue binding domain causes an intramolecular conformational change that restores GFP fluorescence (Fig. 1A). Similar to previous reporters, this reconstitution is excitation ratiometric: GFP emission (~520-nm light) excited by ~488-nm light increases, whereas GFP emission excited by ~405 nm is unchanged or decreases (*37*, *38*). We therefore express CaMKAR signal as the ratio (R) of these two channels (Fig. 1A). To test CaMKAR dynamics, we treated CaMKAR-expressing human embryonic kidney (HEK) 293T cells with ionomycin, causing intracellular Ca^{2+} influx and activation of endogenous CaMKII (Fig. 1, B and C). This resulted in a rapid increase in R relative to baseline (R/R_0). Stimulation with ionomycin in HEK293T cells expressing constitutively active (CA) CaMKII revealed an in cellulo maximal dynamic range of 3.27-fold or 227 ± 11.1% (fig. S1B). Because the 405-nm channel is largely unchanged upon stimulation, CaMKAR can also be used intensiometrically by only quantifying the 488-nm channel intensity; this modality retains 96.4 ± 1.6% of the dynamic range compared with ratiometric mode (fig. S1C). Pretreatment with the ATP-competitive CaMKII inhibitor AS100397 (fig. S1, D and E), a congener of AS105 (*25*, *39*, *40*), eliminates CaMKAR signal, and posttreatment with the Ca^{2+}-chelator EGTA rapidly reduces CaMKAR signal (Fig. 1C). We validated that CaMKAR senses bona fide CaMKII-catalyzed phosphorylation by orthogonal approaches. First, we cotransfected CaMKAR with constructs that express CaMKIIδ variants under a doxycycline-inducible promoter in HEK293T cells: As expected, overexpression of wild-type (WT) CaMKII without Ca^{2+} stimulation led to no change in CaMKAR signal, and expression of CA CaMKII^{T287D}, but not kinase-defective CaMKII^{K43M}, increases CaMKAR signal (Fig. 1D), suggesting that kinase activity is a requirement for CaMKAR signal induction. To ensure that sensing occurs via phosphorylation at the proposed substrate site (threonine-6), we repeated the previous experiment using CaMKAR containing a nonphosphorylatable alanine residue at position 6 (T6A mutation); this mutation completely abolished sensing to both ionomycin stimulation and CA CaMKII^{T287D} (Fig. 1E). Further supporting a phosphorylation-dependent mechanism, ionomycin-stimulated CaMKAR signal was enhanced and failed to resolve when coincubated with the pan-phosphatase inhibitor calyculin A (fig. S1F). Together, these assays support that CaMKAR senses CaMKII activity by direct phosphorylation of threonine-6 and that the CaMKAR signal is reversible via phosphatases. CaMKAR is sensitive to the CA constructs for all four human CaMKII isoforms (α, β, γ, and δ) and the three prevalent splice variants of CaMKIIδ (δC, δB, and δ9) (fig. S1, G and H).

Next, we sought to benchmark CaMKAR′s performance and specificity. Camui was the first CaMKII reporter developed and is still widely used (*33*, *34*). However, it has important limitations: Camui contains and overexpresses brain isoform CaMKIIα and has relatively low dynamic range (~5 to 70% versus CaMKAR′s 227 ± 11.1%), and it reports conformational change rather than enzymatic activity (table S1) (*34*, *41*). In HEK293T cells, CaMKAR displays a nearly 10-fold greater signal-to-noise ratio (fig. S2A) and is about threefold faster (τ_{CaMKAR} = 7.4 versus τ_{Camui} = 21.6; fig. S2B). In cultured rat hippocampal neurons, Camui failed to detect catalytic inhibition of CaMKII, whereas CaMKAR detected both catalytic and allosteric inhibition (fig. S2, C to G). Head-to-head comparison of these reporters in these cells demonstrated that CaMKAR is more sensitive than Camui and another reporter, FRESCA, under the same stimulus (fig. S2, H and I). Thus, CaMKAR appears to have both improved sensitivity and kinetics. Because Ca^{2+}-mobilizing agents can activate many kinases, we set to validate CaMKAR′s specificity. In rat CMs (which highly express endogenous CaMKIIδ), pacing-induced CaMKII activity

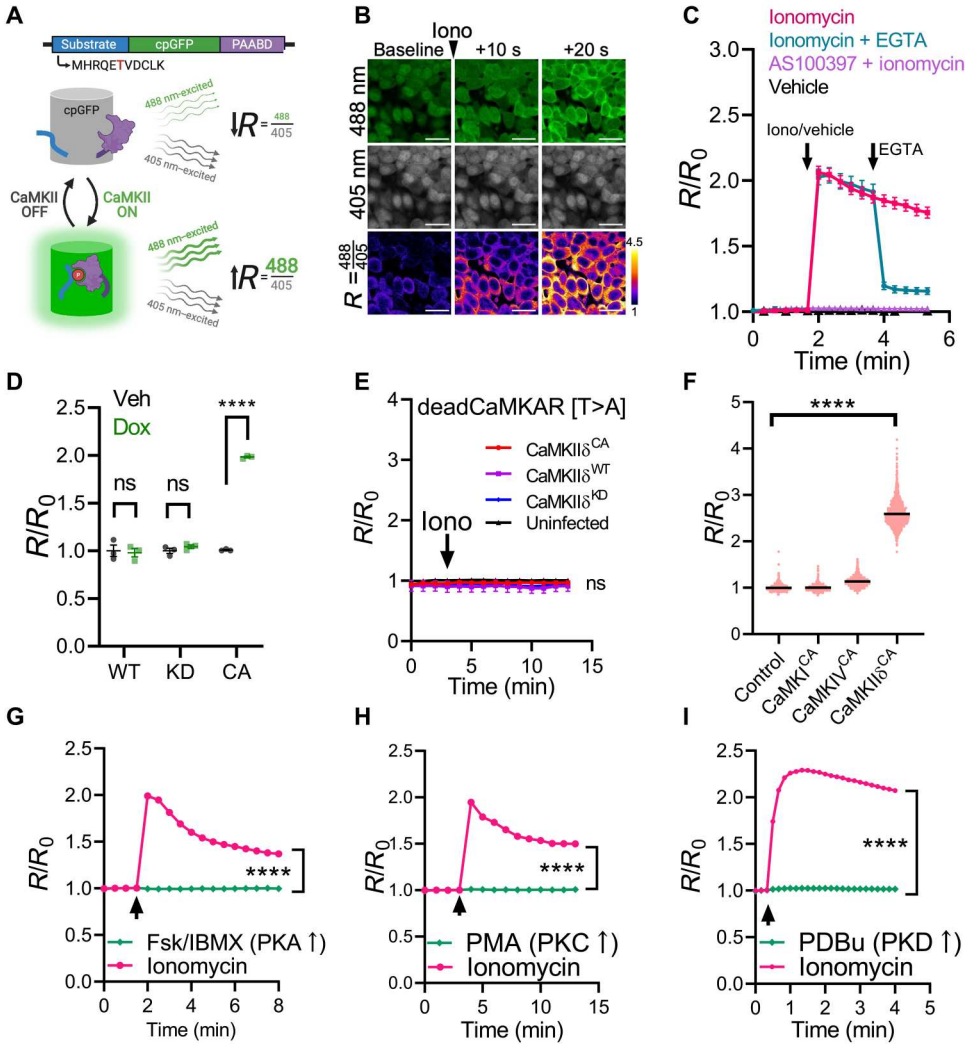

Fig. 1. CaMKAR is a sensitive and specific CaMKII activity reporter. (**A**) Schematic depiction of CaMKII activity reporter (CaMKAR). PAABD, phosphorylated amino acid binding domain). The phospho-substrate threonine is shown in red. Upon phosphorylation by CaMKII, the substrate is bound by the PAABD, which enables conformational reconstitution of GFP fluorescence: 488-nm emission is increased, whereas 405-nm emission is unchanged. (**B**) Fluorescence confocal microscopy of CaMKAR-expressing HEK293T cells treated with ionomycin (5 μM). *R*, ratio of 488 nm–excited (green) and 405 nm–excited intensities (gray). Scale bars, 20 μm. The third row is pseudo-colored to display fold change over baseline. (**C**) Summary data for the CaMKAR signal in HEK293T cells over time treated with vehicle only (black, $n = 2488$ to 2615 cells) or ionomycin (iono; magenta; 5 μM; $n = 1733$ to 2220 cells), pretreatment with the CaMKII inhibitor AS100397 (purple, 10 μM; $n = 1305$ to 1348 cells), or posttreatment with EGTA (teal, 5 mM; $n = 1474$ to 1746). No exogenous CaMKII was added. R/R_0, *R* normalized to mean baseline. Arrows denote administration time. (**D**) CaMKAR signal in HEK293T cells expressing doxycycline-inducible wild type (WT), kinase dead (KD; K43M mutation), or constitutively active (CA; T287D mutation) CaMKIIδ_C compared with vehicle-treated. $N = 3$ wells per condition. (**E**) deadCaMKAR(T6A mutant) signal over time in HEK293T cells coexpressing WT (n = mean of three wells), CA (n = mean of three wells), kinase dead CaMKIIδ_C (KD; n = mean of three wells), or empty vector (n = mean of three wells) and then stimulated with ionomycin. (**F**) CaMKAR signal in CaMKAR-expressing HEK293T cells cotransfected with CA CaMKI ($n = 1471$ cells), CaMKIV ($n = 1732$ cells), or CaMKIIδ ($n = 1816$ cells). (**G**) CaMKAR signal in CaMKAR-expressing HEK293T cells treated with forskolin (Fsk; 50 μM)/IBMX (100 μM; $n = 1834$ to 1891 cells) or ionomycin ($n = 1997$ to 2293). (**H**) CaMKAR signal in CaMKAR-expressing HEK293T cells treated with PMA (100 ng/ml; $n = 696$ to 737 cells) or ionomycin (5 μM; $n = 767$ to 916). (**I**) CaMKAR signal in CaMKAR-expressing HEK293T cells treated with PDBu (200 nM; $n = 1706$ to 1736 cells) or ionomycin (5 μM; $n = 1206$ to 1228). For (G to I), arrows denote administration time of either ionomycin or one of Fsk/IBMX, PMA, and PDBu. Data are shown as means ± SEM (error is not displayed whenever it is smaller than the data point). All observations are taken from more than three biological replicates. ns, $P > 0.05$ and ****$P < 0.0001$; significance was determined via two-way analysis of variance (ANOVA) and Šidák's multiple comparisons test (D and G to I), linear regression (E), and one-way ANOVA with Dunnett's multiple comparisons test (F).

as detected by CaMKAR was abrogated by a 3-day incubation with anti-CaMKIIδ small interfering RNA (fig. S2J). In HEK293T cells, CaMKAR is insensitive to coexpression with CA CaMKI and CaMKIV (Fig. 1F). CaMKAR also failed to sense forskolin/IBMX-mediated cyclic adenosine monophosphate–dependent protein kinase (PKA) activation, phorbol 12-myristate 13-acetate (PMA)–mediated protein kinase C (PKC) activation, and phorbol 12,13-dibutyrate (PDBu)–mediated PKD activation (Fig. 1, G to I). We verified that the concentrations of forskolin/IBMX and PMA used in these studies were sufficient to elicit PKA (fig. S2K) and PKC activity (fig. S2L). Similarly, CaMKAR′s response to ionomycin was unhindered by Gö6976, a dual PKC/PKD inhibitor (fig. S2M).

We leveraged the unique properties of CaMKAR to measure CaMKII activity in vitro. Recombinant CaMKAR is fully functional and exhibits appropriate spectral changes upon incubation with purified CaMKII (fig. S3A). These changes are ATP dependent, further confirming a dependence on phosphorylation for reporter function (fig. S3, A to C). CaMKAR displays a larger dynamic range in vitro (264 ± 2.1%) compared with cell-based assays (227 ± 11.1%), and the rate of the reaction is determined by the amount of CaMKII (fig. S3, D and E). Together, we have demonstrated that CaMKAR is a bona fide CaMKII activity reporter with unprecedented sensitivity, fast kinetics, specificity, and suitability for live-cell and in vitro drug screening.

CaMKAR-based screen of drugs in clinical use

Next, we aimed to canvass the clinically approved pharmacopeia for drugs that are potent CaMKII inhibitors. For high-throughput screening, we first created a stable line of human K562 cells that co-express CaMKAR and CaMKIIδ^{CA}: K562$^{CaMKII\text{-}CaMKAR}$ (Fig. 2A). We chose K562 cells because they grow at high density and remain viable after expression of active CaMKII (fig. S4A). The use of CA CaMKII instead of Ca^{2+}/calmodulin-activated CaMKII increases the likelihood of identifying catalytic inhibitors rather than calmodulin inhibitors (such as KN-93). The sensitivity of CaMKAR enables screening to occur in small culture volumes: CaMKII inhibition by AS100397 is detectable in as little as 30 μl of cell culture (fig. S4B). As our primary screen, we tested this cell line against the Johns Hopkins Drug Library v3.0, constructed by pooling 4475 compounds approved for human use by regulatory agencies from the United States, Europe, Japan, and China. This library targets 44 different pathway families and contains more than 100 kinase inhibitors (data file S1). After 12 hours of treatment, cells were assayed for CaMKAR signal using high-content imaging. Among drugs with an inhibitory signal, we found 118 compounds that reduced CaMKII activity by 60% or more, using a false discovery–adjusted P value cutoff of $<3 \times 10^{-5}$ (Fig. 2B and data file S1). We reasoned that these hits likely contained a mixture of genuine inhibitors and false positives (such as autofluorescent compounds, indirect inhibitors, and phosphatase activators). To discern true inhibitors from false positives, we performed a secondary screen using our recombinant CaMKAR in vitro assay as described in fig. S3. In this assay, we measured fluorescence in a mixture of CaMKII, Ca^{2+}-bound calmodulin (Ca^{2+}/CaM), and CaMKAR at baseline, after drug addition and after catalysis was initiated with ATP. Thus, this screen could help determine whether a drug was autofluorescent and/or a direct inhibitor. Our assay revealed 13 compounds with meaningful inhibition of CaMKII activity (Fig. 2C and data file S2). Both screening steps returned our positive control, pan-kinase inhibitor staurosporine. To remove weak inhibitors and further validate our results, these compounds were tested with HEK293T cells coexpressing CaMKAR and CaMKIIT287D in our laboratory (fig. S5) and in vitro by an independent commercial laboratory (data file S2). These combined results identified five potent CaMKII inhibitors—ruxolitinib, crenolanib, baricitinib, abemaciclib, and silmitasertib—which are all known to be ATP-competitive kinase inhibitors (Figs. 2D and fig. S6). None of the compounds were designed against kinases in the CAMK superfamily, and three of the five compounds are intended against tyrosine kinases, one of the most dissimilar kinase families to CAMK by kinase domain homology (Fig 2D). Unlike KN-93 (*23*), all five compounds inhibited Ca^{2+}-independent, autonomously hyperactive CaMKII in HEK293T cells (Fig. 2E, left). In this assay, crenolanib, ruxolitinib, abemaciclib, and baricitinib were more potent than AS100397, and all drugs except crenolanib were less cytotoxic after a 12-hour exposure (Fig. 2E, right). Thus, ruxolitinib, abemaciclib, and baricitinib appeared to be more potent and less toxic than our tool compound in cultured cells.

Clinically approved drugs inhibit CaMKII in cardiac cells

Because of the established benefits of CaMKII inhibition in cardiovascular disease models, we asked whether these five compounds could inhibit CaMKII in CMs. In neonatal rat ventricular myocytes (NRVMs), we can stimulate CaMKII activity by rapid field pacing (Fig. 3, A and B). Preincubation of all five compounds inhibited this response at high doses (Fig. 3C). However, to determine which compounds are likely to have an effect at clinically achievable doses, we adjusted each concentration to their respective maximal human plasma concentrations (*42*–*46*). This revealed that ruxolitinib, crenolanib, abemaciclib, and silmitasertib, but not baricitinib, sustained inhibition (Fig. 3, D and E). Because of its high potency and low toxicity and favorable safety profile among our hits (table S2), we henceforth focused on ruxolitinib. We then ascertained that ruxolitinib is capable of inhibiting preactivated CaMKII, returning activity to baseline within 30 s in CMs that began pacing before drug administration (Fig. 3F). Head-to-head comparison shows that ruxolitinib is more than 10-fold more potent than DiOHF (Fig. 3G) (*29*, *30*). This inhibitory effect appears to be independent of ruxolitinib′s Janus kinase 1/2 (JAK1/2) inhibition. For one, we found multiple JAK1/2 inhibitors in our screen that failed to reduce the CaMKAR signal (fig. S7A). Among these compounds, their known IC_{50} values against JAK1/2 did not significantly correlate ($P = 0.85$ for JAK1 and $P = 0.11$ for JAK2) with CaMKAR signal inhibition in our screen (fig. S7B). Filgotinib, another FDA-approved drug with similar potency against JAK1/2, failed to inhibit pacing-induced CaMKII activity (fig. S7C). Last, an in vitro biochemical assay with recombinant CaMKII protein confirmed inhibition of CaMKII with ruxolitinib in the absence of JAK1/2 with an inhibitory constant (K_i) of 23.4 ± 2.18 nM (compared with DiOHF, which has a published IC_{50} of 250 nM) and an ATP-competitive mechanism (fig. S7D). Forty-eight–hour exposure in NRVMs revealed that ruxolitinib is well tolerated up to 100 μM, which was similar to DiOHF and superior to KN-93 and AS100397 (Fig. 3H). We conclude that the drugs identified in our screen can inhibit CaMKII in cardiac cells, but among these, ruxolitinib appears to be best suited for repurposing because of its potency and low toxicity.

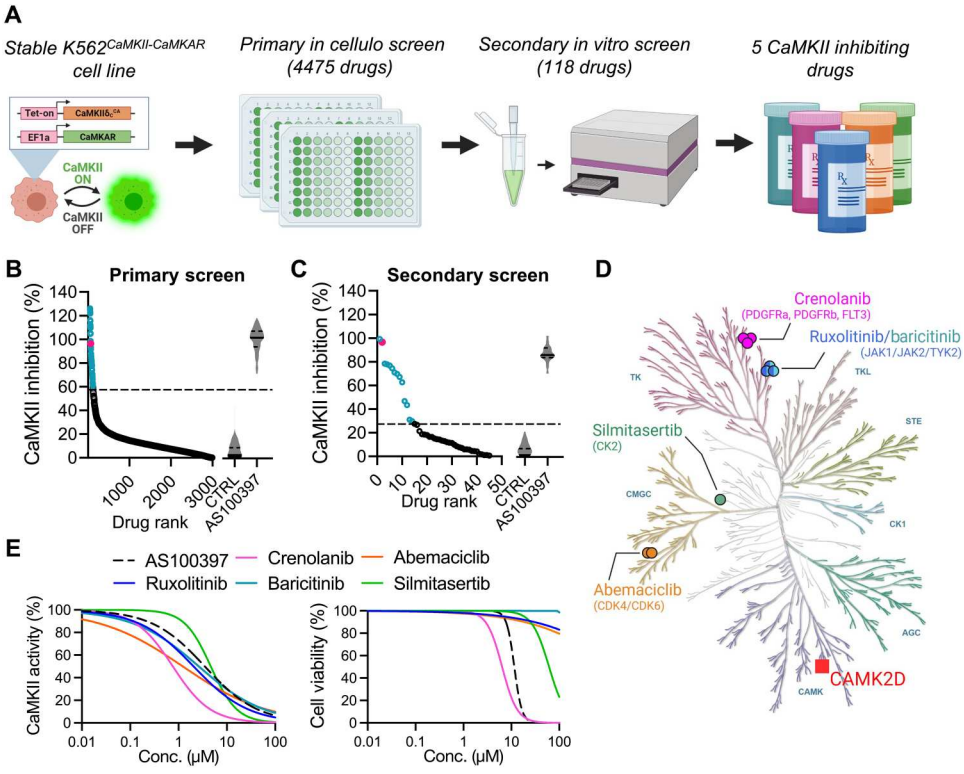

Fig. 2. CaMKAR-based screen identifies CaMKII inhibitors among drugs in clinical use. (**A**) Schematic depiction of CaMKAR-based high-throughput screen. K562 cells were coinfected with CaMKAR- and CA CaMKIIδ^{T287D}–encoding lentiviruses. CaMKII expression could be induced with doxycycline. K562$^{CaMKII\text{-}CaMKAR}$ cells were screened against the Johns Hopkins Drug Library v3.0. Primary hits were further screened using in vitro assays to eliminate false positives and narrow the list to five CaMKII inhibitors. (**B**) Drugs ranked according to in cellulo CaMKII inhibition in primary screen. CaMKII inhibition percentage defined by minimum-maximum normalization using means of control groups [CTRL (untreated) and AS100397; same data as fig. S4B]. A total of 118 selected hits are shown in blue. Positive control staurosporine is shown in magenta. The dashed line represents hit selection threshold (see Materials and Methods). Data shown are subsets (those scoring between 0 and 140% for visualization of hits) from the complete dataset in data file S1. (**C**) Hits from (B) ranked according to in vitro CaMKII inhibition as detected by CaMKAR secondary screen. CaMKII inhibition normalized against untreated control (CTRL). AS100397 was used as a positive control. Thirteen identified hits are in blue. Staurosporine is shown in magenta. Data shown are subsets from the complete dataset (see Supplementary Materials). (**D**) Five CaMKII inhibitory drugs and their intended targets within the human kinase homology dendrogram. Kinase families: AGC, containing PKA, PKG, and PKC families; CK1, casein kinase 1; CMGC, containing CDK, MAPK, GSK3, and CLK; STE, homologs of yeast sterile 7, sterile 11, and sterile 20; TK, tyrosine kinase; TKL, tyrosine kinase–like. (**E**) IC_{50} (left) and cell viability (right) curves from 293T cells expressing CaMKAR and CaMKII^{T287D} and exposed to five candidate drugs and CaMKII inhibitor (AS100397, 10 mM). Measurements in (E) are done in biological triplicate; complete dataset is shown in fig. S5.

We then evaluated whether ruxolitinib could also inhibit CaMKII activity in vivo. Ten-minute systemic pretreatment with ruxolitinib at 41, 75, and 180 mg/kg suppressed isoproterenol-induced phosphorylation of phospholamban at threonine-17, a validated marker of CaMKII activity (*47*–*49*), in a concentration-dependent manner (Fig. 4, A to C). This dosing range was chosen because doses at 30 to 180 mg/kg have been used for JAK inhibition in mice (*50*–*54*), and doses at 60 to 90 mg/kg have been reported to be analogous to the prescribed 20 to 25 mg in humans (see Discussion for limitations) (*51*–*53*). Together, our data demonstrate that ruxolitinib can inhibit CaMKII in CMs and functions rapidly in vivo.

Ruxolitinib inhibits arrhythmias in mouse and patient-derived models

Given its robust inhibition of CaMKII in cellulo and in vivo, we tested whether ruxolitinib can ameliorate CaMKII-associated cardiac pathology. We first examined CPVT because CaMKII hyperactivity plays an essential role in this arrhythmia (*10*, *11*, *13*, *55*). We isolated peripheral blood mononuclear cells from a patient with recurrent exercise-induced arrhythmia and a dominant mutation in the ryanodine receptor type 2 (*RYR2*$^{S404R/WT}$) for reprogramming into induced pluripotent stem cells (iPSCs) (*15*). After differentiation into functional CMs (iPSC-CMs), we performed steady-rate electrical pacing at 1 Hz for 10 s, followed by cessation of pacing during continuous Ca^{2+} imaging. The frequency of spontaneous abnormal Ca^{2+} release events (aCREs) after the cessation of pacing reflects the cellular mechanism for CPVT and is markedly increased in iPSC-CMs with pathogenic CPVT mutations (Fig. 5A). Preincubation with ruxolitinib effectively suppressed aCREs in *RYR2*$^{S404R/WT}$ iPSC-CMs compared with vehicle only (Fig. 5B). Automated analysis of Ca^{2+} transients during steady-rate pacing did not reveal any effects on peak Ca^{2+} amplitude (Fig. 5C), transient duration (Fig. 5D), or upstroke velocity (Fig. 5E). In addition, ruxolitinib treatment normalized the downstroke velocity of paced Ca^{2+} transients *RYR2*$^{S404R/WT}$ iPSC-CMs to WT values (Fig. 5F). We also investigated the effects of the other drugs identified by our screen to test whether any were superior

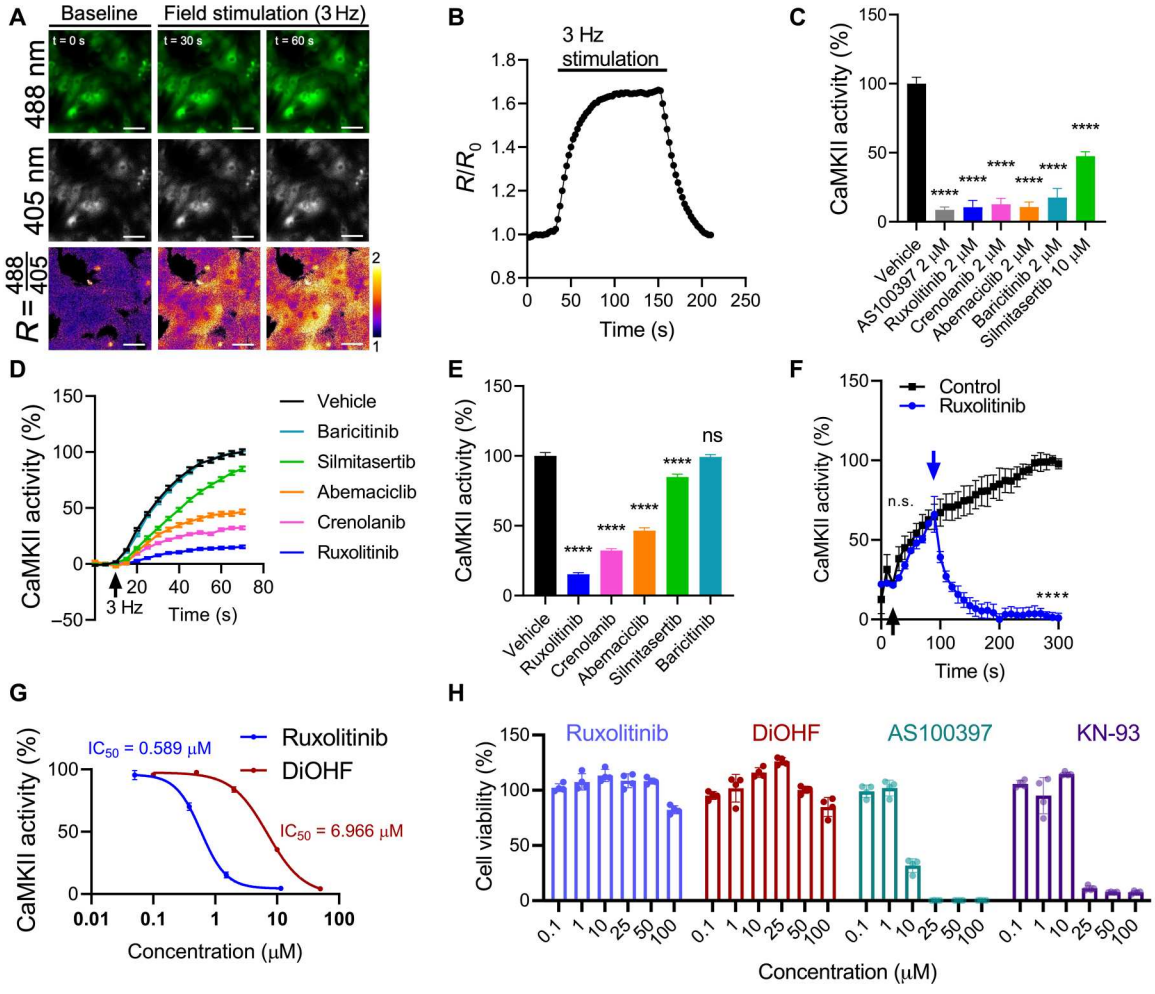

Fig. 3. CaMKAR indicates that drugs in clinical use inhibit CaMKII in CMs. (**A**) Fluorescence imaging time lapse (0, 30, and 60 s) of CaMKAR-expressing neonatal rat ventricular CMs (NRVMs) and (**B**) summary data during 3-Hz field pacing (n = 1065 to 1160 cells). R, ratio of 488 nm–excited and 405 nm–excited intensities. Third row of images is pseudo-colored to display fold change over baseline. R/R_0, R normalized to mean R before stimulation. Scale bars, 50 μm. (**C**) Effect of treatment with vehicle (n = 317 cells), AS100397 (n = 151), ruxolitinib (n = 148), crenolanib (n = 156), abemaciclib (n = 138), baricitinib (n = 136), and silmitasertib (n = 149) on pacing-induced CaMKII activity in NRVMs. CaMKII inhibition percentage defined by minimum-maximum normalization between untreated and maximally stimulated CaMKAR signal. (**D**) CaMKII inhibition over time in NRVMs treated with drugs adjusted to their maximum human plasma concentrations during 3-Hz pacing: ruxolitinib (1.51 μM, n = 384 cells), crenolanib (478 nM, n = 302), abemaciclib (243 nM, n = 302), baricitinib (58 nM n = 334), and silmitasertib (3.42 μM, n = 285). The arrow indicates start of pacing. (**E**) Summary data from (D) at 60 s after stimulation. (**F**) Analysis of CaMKII activity based on CaMKAR time-lapse imaging in NRVMs treated with ruxolitinib after initiation of pacing and CaMKII activation. Black arrow denotes pacing start; blue arrow denotes addition of ruxolitinib (n = 3 wells) or control vehicle (n = 3 wells). (**G**) IC_{50} curves for ruxolitinib (n = 308 to 384 per data point) and DiOHF (n = 305 to 363) in NRVMs against pacing-induced CaMKII activity. (**H**) Cell viability after 48-hour compound incubation. All measurements were taken from more than three biological replicates. ns, $P > 0.05$ and ****$P < 0.0001$; significance determined via one-way ANOVA and Dunnett's multiple comparisons test (C and E) and two-way ANOVA and Tukey's multiple comparisons test (F).

to ruxolitinib in reversing this disease phenotype. Among these, ruxolitinib was the best at suppressing aCREs in $RYR2^{S404R/WT}$ iPSC-CMs (fig. S8A) and restoring Ca^{2+} transient parameters (fig. S8, B to E).

Arrhythmias are emergent properties of tissues and not just single cells. Thus, we next focused on a validated mouse model of CPVT. Mice with the knock-in mutation $Ryr2^{R176Q}$ have spontaneous and inducible ventricular arrhythmias in response to adrenergic stimulation and ventricular pacing (*56*). To first test that ruxolitinib could suppress the single-cell arrhythmogenic phenotype in the $Ryr2^{R176Q/WT}$ genotype, we isolated adult CMs from WT and mutant mice. Similar to iPSC-CMs derived from a patient suffering from CPVT, $Ryr2^{R176Q/WT}$ adult CMs demonstrated aCREs after the cessation of steady-rate pacing (Fig. 6A). Preincubation for 10 min with 2 μM ruxolitinib significantly reduced the frequency of these events in the $Ryr2^{R176Q/WT}$ adult CMs [dimethyl sulfoxide (DMSO) versus ruxolitinib-treated, P = 0.0002; Fig. 6, A and B]. To investigate the effects of ruxolitinib on ventricular arrhythmias in CPVT in vivo, we treated WT and $Ryr2^{R176Q/WT}$ mice with either ruxolitinib at a dose of 75 mg/kg or vehicle alone (DMSO) by peritoneal injection 10 min before electrophysiology testing. Programmed electrical stimulation from the right ventricle induced episodes of polymorphic and monomorphic ventricular tachycardia in $Ryr2^{R176Q/WT}$ animals treated with vehicle only (Fig. 6C). However, animals

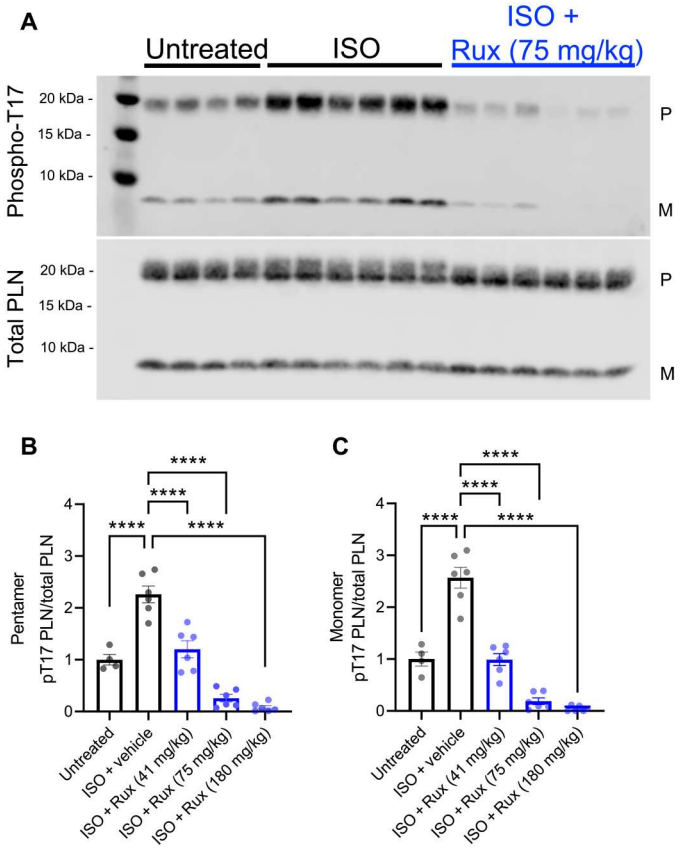

Fig. 4. Ruxolitinib inhibits CaMKII in vivo. (**A**) Immunoblot and (**B** to **C**) quantitation of phospholamban (PLN; pentameric or monomer) and threonine-17–phosphorylated phospholamban in whole-heart lysates from mice treated with intraperitoneal ruxolitinib (Rux) for 10 min before isoproterenol (ISO) stimulation. P, pentameric PLN; M, monomeric PLN. Data points represent individual mice. ****$P < 0.0001$; significance determined via one-way ANOVA and Tukey's multiple comparisons test.

treated with ruxolitinib demonstrated a substantial reduction in the frequency of induced ventricular arrhythmias (Fig. 6, C and D). Furthermore, the duration of induced arrhythmias in CPVT mice were also significantly reduced with ruxolitinib treatment (vehicle versus ruxolitinib-treated, $P = 0.0103$; Fig. 6E). Consistent with known effects of CaMKII inhibition (*2*), ruxolitinib suppressed the adrenergic-induced heart rate increase (fig. S9, A to C). No other electrophysiology parameters were negatively affected (table S3). To confirm that ruxolitinib inhibited CaMKII in our CPVT model, we made whole-heart lysates from animals immediately after electrophysiology testing. Similar to above, ruxolitinib at a dose of 75 mg/kg significantly inhibited CaMKII-mediated phosphorylation at threonine-17 of phospholamban (vehicle versus ruxolitinib treated, $P = 0.0042$; fig. S10).

Next, we tested whether ruxolitinib can prevent and rescue acquired arrhythmia. CaMKII is a pivotal proarrhythmic signal in AF (*57*–*59*). Diabetes is a known risk factor for AF, thought to be in part due to hyperglycemia-induced CaMKII activation (*60*, *61*). We have previously shown that genetic and chemical interventions that reduced CaMKII activity suppressed AF in diabetic mice (*59*). Here, we also found that a 10-min pretreatment of hyperglycemic mice with ruxolitinib (75 mg/kg) abolished pacing-induced AF (Fig. 7, A and B). Examination of threonine-17–phosphorylated phospholamban in atria from these mice confirmed suppression of CaMKII activity in ruxolitinib-treated mice (fig. S11). In *O*-GlcNAc (*N*-acetylglucosamine) transferase (OGT)–overexpressing mice, which develop dilated cardiomyopathy and have increased arrhythmic burden (*62*), ruxolitinib similarly prevented pacing-induced AF (Fig. 7C). Last, we tested for rescue of ongoing arrhythmia using CREM-IbΔC-X transgenic mice, a validated model of spontaneous AF; by 7 months of age, >70% of CREM-IbΔC-X mice develop persistent AF (*63*, *64*). Ten minutes after ruxolitinib treatment, mice showed reduced percentage of time in AF to 33.63 ± 6.5% compared with times of those treated with vehicle, which remained at 95.24 ± 3.65% (Fig. 7, D and E). Collectively, these data support that ruxolitinib can effectively inhibit CaMKII in both atrial and ventricular myocardium and suppress arrhythmogenesis in experimental models of inherited and acquired arrhythmia.

Ruxolitinib does not lead to short-term or spatial memory deficits

CaMKII is well known for its role in learning and memory (*65*). Hence, cognitive off-target effects have been a major criticism against developing CaMKII inhibitors for human use (*24*). Ruxolitinib is inefficient at crossing the blood-brain barrier, with brain concentration being 29-fold lower than plasma concentration in rats (*66*). Furthermore, ruxolitinib has been prescribed to patients for over a decade without reported overt cognitive deficits (*67*). Thus, we hypothesized that there may be a therapeutic window where efficient cardiac inhibition can be achieved without impairing cognition. To test whether this was the case in our models, we treated mice with ruxolitinib and subjected them to the novel object recognition test (NORT) and the Y maze spatial memory test (Fig. 8A), two established behavioral paradigms that test spatial short-term memory. These were chosen because CaMKII inhibition is known to affect both short-term and spatial memory (*68*–*70*), and numerous studies observe robust deficits in novel object recognition upon CaMKII inhibition (*68*, *71*–*74*). Neither single dose (1 hour before) nor multiple doses (twice daily for 7 days) of ruxolitinib (75 or 41 mg/kg) caused significant differences in novel object recognition ($P = 0.56$ and $P = 0.68$), as measured by percentage of time spent with the novel object (Fig. 8, B and C). Total distance traveled during testing was similar for both groups, confirming equivalent locomotion (Fig. 8, D and E). In the Y maze test, single dosing using the lower dose showed decreased preference for the novel arm (Fig. 8F), but this effect was not seen in the higher dose or in either of the multiple dosing cohorts (Fig. 8, F and G).

To assess longer-term spatial memory formation, we tested the effect of ruxolitinib treatment on Barnes maze performance, a test that is also validated to detect CaMKII disruption (*69*). Mice were initiated on ruxolitinib (150 mg/kg per day) 1 day before training and were maintained on treatment throughout the entire study to ensure continuous exposure to drug (fig. S12A). At the study end point, there was no difference in maze-solving latency between the treatment or vehicle groups (fig. S12B). During the training trials, there was no significant effect in latency ($P = 0.57$), primary errors ($P = 0.34$), and total errors ($P = 0.42$) due to ruxolitinib treatment; reassuringly, all three parameters were significantly decreased across days ($P < 0.0001$, $P = 0.0037$, and $P < 0.0001$), demonstrating adequate learning (fig. S12, C to E). These results suggest that, at

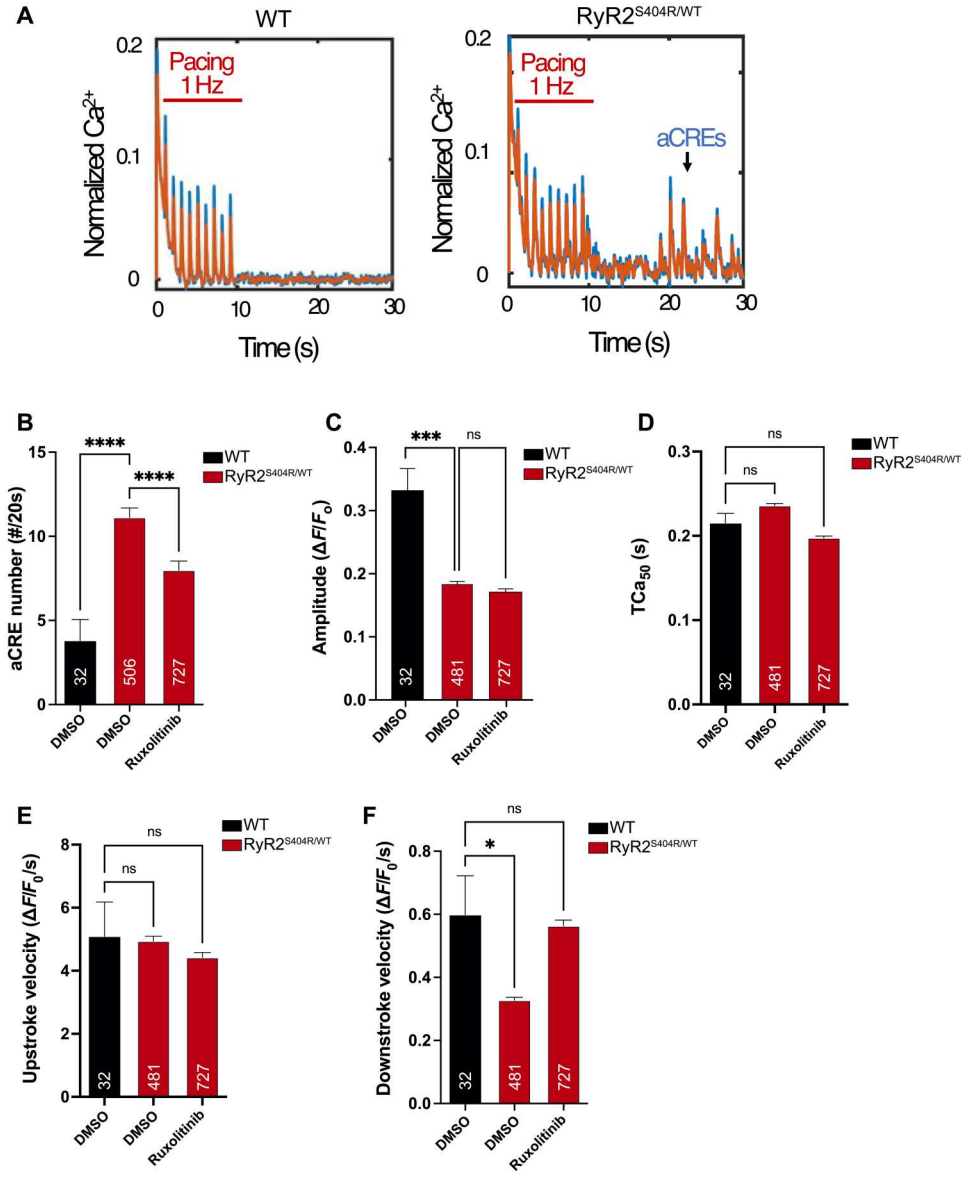

Fig. 5. Ruxolitinib suppresses abnormal calcium signaling in a cellular model of CPVT. iPSCs with the dominant *RYR2* mutation (p.S404R) were generated from a patient with a clinical diagnosis of CPVT (*RYR2*$^{S404R/WT}$) and differentiated into functional CMs (iPSC-CMs). After plating on glass-bottom dishes, *RYR2*$^{S404R/WT}$ and WT iPSC-CMs were loaded with the fluorescent Ca^{2+} indicator (Fluo-4) and electrically paced at 1 Hz for 10 s. (**A**) Representative tracings of calcium transients in WT and *RYR2*$^{S404R/WT}$ cells. The appearance of aCREs after the cessation of pacing is indicative of deranged Ca^{2+} signaling in CPVT iPSC-CMs (right). Raw data are in blue, and filtered data are in orange overlay. (**B**) Quantification of aCREs over 20 s in WT and *RYR2*$^{S404R/WT}$ iPSC-CMs with preincubation of 2 μM ruxolitinib compared with vehicle alone (DMSO). (**C** to **F**) Automated analysis of Ca^{2+} transient parameters during 1-Hz pacing of iPSC-CMs for mean amplitude (C), Ca^{2+} transient duration at 50% of peak amplitude (TCa_{50}) (D), upstroke velocity (E), and downstroke velocity (F). The numbers of analyzed cells (*n*) are annotated on each graph and were from at least two independent differentiations and four separate culture wells. Statistics were performed by one-way Kruskal-Wallis with Dunn's multiple comparisons test: ns, $P > 0.1$; *$P < 0.05$; **$P < 0.01$; ***$P < 0.005$; and ****$P < 0.0001$.

tested doses, ruxolitinib did not lead to detectable impairment of short-term or spatial memory, demonstrating that it may be possible to limit cardiac CaMKII activity without substantial memory impairment in mice.

DISCUSSION

In this work, we developed and validated CaMKAR, a fluorescent CaMKII activity reporter uniquely suited for high-throughput screening. CaMKAR displays the highest dynamic range of all CaMKII reporters to date; a high degree of specificity; and versatility afforded by ratiometric, intensiometric, and in vitro functionality. We demonstrated these properties by screening a collection of clinically approved compounds as possible CaMKII inhibitors. Our

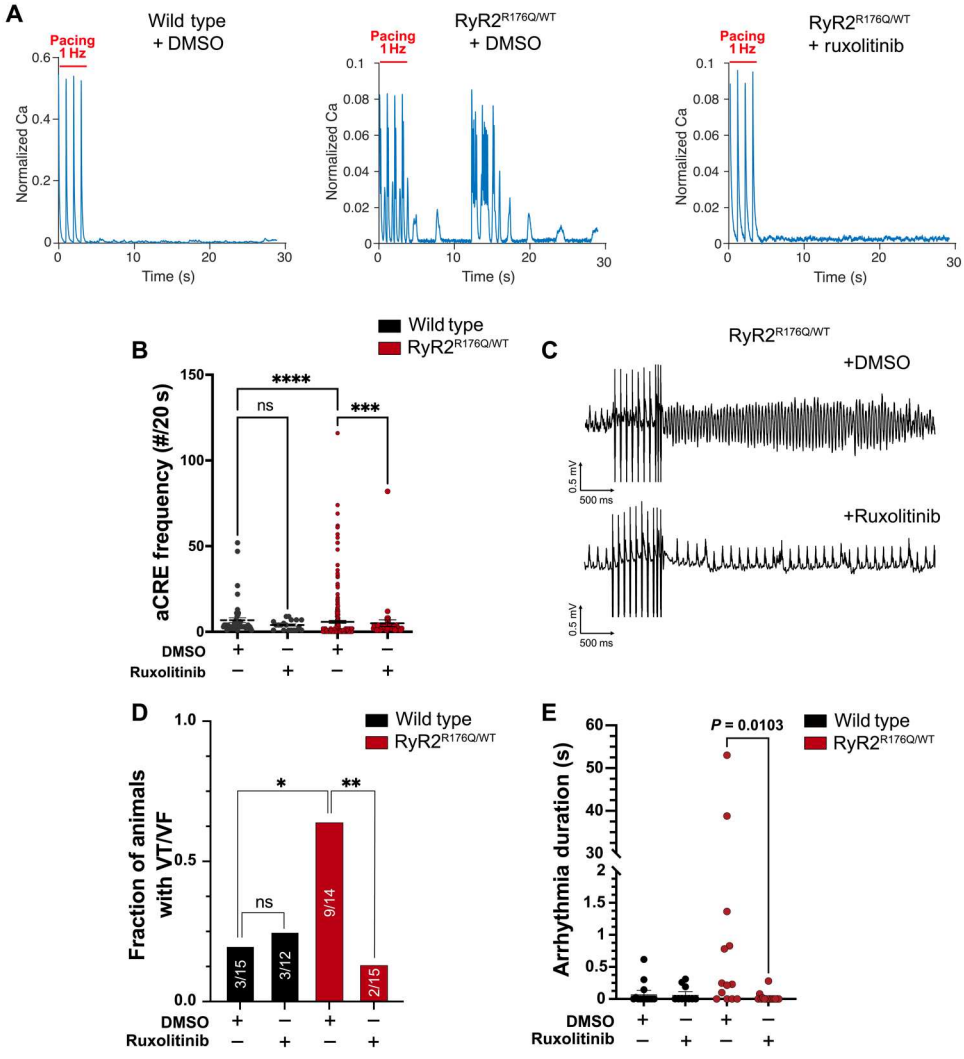

Fig. 6. Ruxolitinib prevents arrhythmias in a murine model of CPVT. Isolated adult murine CMs from mice with the pathogenic CPVT variant *Ryr2*$^{R176Q/WT}$ were loaded with the calcium indicator Rhod-2 and paced for 30 s at 1 Hz. (**A**) Representative tracings of calcium transients in WT and *Ryr2*$^{R176Q/WT}$ CMs treated with DMSO or ruxolitinib. (**B**) Quantification of aCRE frequency over 20 s for WT and *Ryr2*$^{R176Q/WT}$ CMs after preincubation with 2 μM ruxolitinib (or DMSO). (**C**) Animals were treated with ruxolitinib (75 mg/kg) or vehicle by intraperitoneal injection and then subjected to programmed ventricular extrastimulus testing. Representative traces of induced ventricular arrhythmias *Ryr2*$^{R176Q/WT}$ animals with vehicle- but not in ruxolitinib-treated mice. (**D**) Quantification of animals with ventricular arrhythmias (VF/VT) in WT and *Ryr2*$^{R176Q/WT}$ animals with vehicle or ruxolitinib treatment after concurrent stimulation with isoproterenol (2 mg/kg) and epinephrine (4 mg/kg). (**E**) Quantification of the duration of arrhythmias induced by ventricular pacing in WT and *Ryr2*$^{R176Q/WT}$ animals with vehicle or ruxolitinib treatment. Number of animals in each group (*N*): *N* = 13 (WT + DMSO), *N* = 10 (WT + ruxolitinib), *N* = 13 (*Ryr2*$^{R176Q/WT}$ + DMSO), and *N* = 15 (*Ryr2*$^{R176Q/WT}$ + ruxolitinib). Statistics were performed by one-way Kruskal-Wallis with Dunn's multiple comparisons test, for continuous variables or chi-squared for discrete variables: ns, $P > 0.1$; *$P < 0.05$; **$P < 0.01$; ***$P < 0.005$; and ****$P < 0.0001$.

data revealed that CaMKII inhibitors already exist in the human pharmacopeia and that FDA-approved ruxolitinib may be a candidate for cardiovascular repurposing.

This work has several limitations. First, it remains to be determined whether ruxolitinib will have an effect on CaMKII in humans at safely tolerated doses. Although our in vitro and in cellulo data support that achievable concentrations will have an effect, our in vivo data are based on several assumptions. Dosing at 60 to 90 mg/kg has been previously reported to be analogous to human 20- to 25-mg doses (*51*–*53*), but these studies lack definitive pharmacological data to demonstrate this equivalency. The widely used Nair and Jacob scale (*75*) estimates that the mouse equivalent of 25 mg is ~5 mg/kg, a dose that is too low for an effect in our hands. However, the maximally tolerated human dose of 200 mg (*42*, *76*) yields a mouse dose of ~40 mg/kg, which is within an order of magnitude of our in vivo dosing. Nevertheless, the Nair and Jacob method is a "rule-of-thumb" approach, and it highlights that efficacy in humans will require empirical determination in clinical studies. In addition, chronicity and duration of effect might vary in humans based on route of administration and differences in drug metabolism across species. Although our study used systemic intraperitoneal delivery, ruxolitinib is currently administered orally, with >95% availability (*77*). In our system, we only evaluated short-term inhibition of CaMKII (10 to 25 min after delivery), and the duration of inhibition remains to be determined. Last, our behavioral results support a lack of neurocognitive effects at cardioprotective doses,

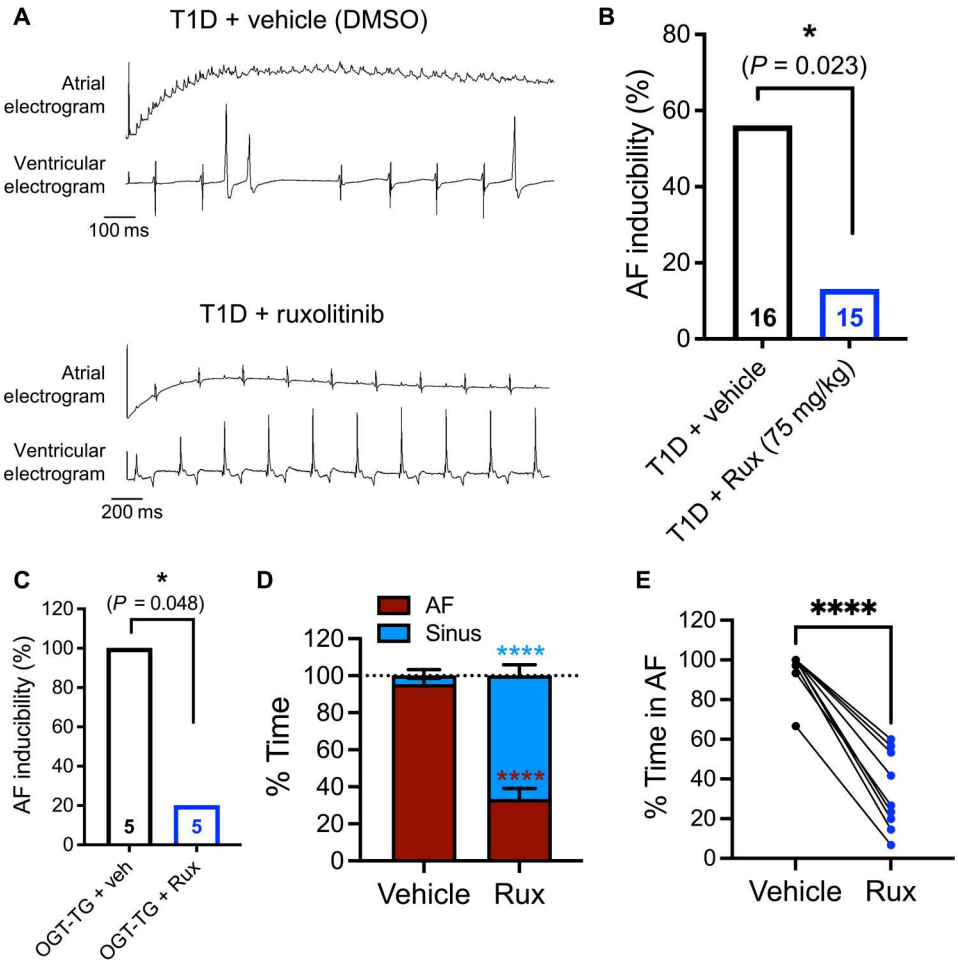

Fig. 7. Ruxolitinib prevents and rescues AF in mice. (**A**) Representative type 1 diabetic mouse tracings immediately after atrial burst pacing. DMSO-treated mice demonstrate AF (top), whereas ruxolitinib (Rux)–treated mice (75 mg/kg; single dose 10 min before, intraperitoneal) retain sinus rhythm (bottom). (**B**) AF inducibility percentage from mice in (A). The total number of mice analyzed per group is shown in each column: Nine of 16 vehicle-treated mice had AF versus 2 of 15 Rux-treated mice. (**C**) Sequential AF (AF) inducibility in OGT-transgenic mice. Mice were treated with vehicle immediately before AF induction; the same mice were then treated with ruxolitinib (75 mg/kg) before pacing for a second time. The number of mice analyzed per group is shown in each column (vehicle, five of five had AF; Rux, one of five had AF). (**D**) Percentage of time in AF or sinus rhythm (for 10 to 25 min after treatment administration) in CREM-IbΔC-X mice when treated with vehicle (baseline) or when treated with ruxolitinib (75 mg/kg) 24 hours later ($n = 9$, paired). (**E**) Individual trajectories of percentage of time in AF (for 10 to 25 min after treatment) in same mice as in (D) ($n = 9$, paired). Statistical comparisons were performed using two-tailed Fischer's exact test (B and C), two-way ANOVA with Šidák's multiple comparison's test (D), and paired Student's *t* test (E); *$P < 0.05$ and ****$P < 0.0001$.

but these assays do not exclude effects in the immediate term (which includes the window of activity confirmed in this study) or after chronic therapy. Despite its poor blood-brain barrier penetrance (*66*), ruxolitinib has been reported to modulate astroglial inflammation in mouse brains (*78*). Therefore, although no memory deficits have been reported in patients, focused clinical studies will be necessary to determine whether subtle neurocognitive effects occur.

To demonstrate translational potential, we focused on CPVT and AF, two diseases driven by CaMKII hyperactivity (*13*, *55*–*59*, *79*–*81*). In both patient-derived human CMs and in mice, ruxolitinib displayed near-complete prevention of arrhythmic phenotypes and a normalization of Ca^{2+} handling. We are hopeful that the therapeutic potential shown here can rapidly translate into patients for two main reasons. First, CPVT murine knock-in models harboring human disease mutations in RyR2 closely recapitulate human responses to stress (*56*). Second, the CaMKII-RyR2-dependent mechanism in CPVT and AF is also shared by numerous arrhythmogenic conditions, including inherited (Timothy syndrome, Duchenne's muscular dystrophy, and ankyrin B mutations) and acquired (such as glycoside toxicity, heart failure, and alcoholic cardiomyopathy) diseases (*5*).

Although animal studies have repeatedly demonstrated that CaMKII blockade is cardioprotective, pharmaceutical companies have remained cautious about developing CaMKII inhibitors because of its pivotal role in memory (*65*). Our results suggest that several drugs already in circulation, taken by thousands to millions of patients, can inhibit CaMKII. Our findings, particularly in regard to ruxolitinib, support a reinvigoration of CaMKII inhibitor development and demonstrate that cardiac CaMKII blockade without impairing cognition may be possible with small molecules.

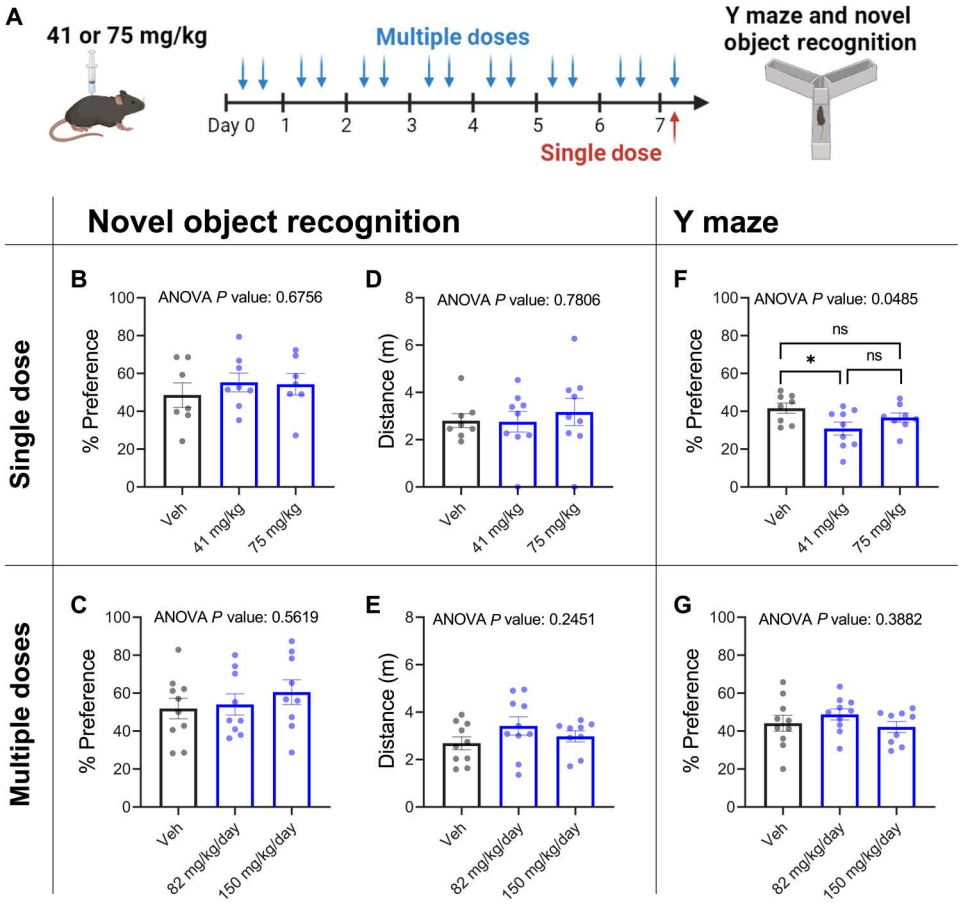

Fig. 8. Ruxolitinib does not impair short-term or spatial memory in mice. (**A**) WT C57BL/6J mice were treated with a single dose (1 hour before) or multiple doses (7 days, twice daily) of ruxolitinib before behavioral testing via the NORT and the Y maze spatial recognition memory test. (**B** and **C**) Percentage of time spent with novel object. (**D** and **E**) Total distance traveled while in the testing chamber. (**F** and **G**) Percentage of time spent in novel arm of Y maze. Each data point represents a mouse (n = 7 to 10 mice for all conditions). ns, $P > 0.05$ and $^*P < 0.05$; significance was determined by one-way ANOVA and Tukey's multiple comparisons test.

FDA-approved screens hold exciting potential for drug repurposing; nevertheless, FDA approval for an original indication does not guarantee approval for other indications. Thus, excitement for repurposing must be tempered with careful evaluation of ruxolitinib's side effect profile, particularly because our biochemical data suggest that CaMKII and JAK1/2 inhibition will be concomitant. Systemic ruxolitinib is used to treat polycythemia vera, myelofibrosis, and splenomegaly. Because of JAK1/2 inhibition, prolonged treatment can result in herpes zoster infection and reversible anemia and thrombocytopenia (*82*, *83*). Encouragingly, two large-scale cohorts of patients taking long-term ruxolitinib (median exposures of 12.4 and of 34.4 months) determined that few patients discontinue treatment because of anemia (<2.6%) or thrombocytopenia (<3.6%) (*82*, *83*). Concern for adverse effects can be abrogated by limiting exposure length, and in agreement with this, ruxolitinib is well tolerated at up to 200 mg in healthy volunteers in single or short-term dosing (*42*, *84*). Thus, we predict that repurposing will be most readily applicable for indications that require short treatment courses because these likely offer the optimal trade-off between CaMKII inhibition and mitigation of undesirable JAK1/2 effects. We have identified three unmet clinical scenarios that match these criteria. One is postoperative AF, which affects 20 to 40% of cardiac surgery patients and is independently associated with increased mortality, length of stay, and health care cost (*85*). A majority of cases happen within 3 days, and >90% happen by day 6 after surgery (*85*, *86*). Another indication could be postmyocardial infarction ventricular tachycardia, a considerable source of peri-infarct mortality, which also occurs predominantly (90%) within the first 48 hours (*87*). A final setting would be cardiac electrical storm, whereby patients experience multiple episodes of ventricular tachycardia and fibrillation within 24 to 48 hours. All three conditions are exacerbated by CaMKII (*88*–*90*), feature β-adrenergic blockade as a mainstay therapy, which has been shown to be insufficient to block CaMKII in human biopsies (*14*), and occur within short and predictable time frames where a short course of ruxolitinib would be feasible. Other experimental CaMKII-modifying modalities, such as antisense oligonucleotides and inhibitor-encoding gene therapy, take effect in the order of days to weeks, which lessens their utility in these acute indications. We demonstrated that ruxolitinib can inhibit preactivated CaMKII and rescue ongoing arrhythmia, which supports a therapeutic role for ruxolitinib as a "pill-in-the-pocket" for AF.

Despite its impressive mechanistic response to CaMKII inhibition in animal models, there are no current CaMKII-inhibiting or

disease-specific therapies available for CPVT. Although the recent addition of flecainide therapy has ameliorated arrhythmic events in many patients, a substantial fraction are refractory to flecainide therapy, experience breakthrough events, and die from sudden arrhythmia despite maximal medical therapy and use of implantable cardiac defibrillators (ICDs). The use of ICDs is associated with potentially lethal ICD storms and death in some patients with exhausted therapies (*91*). Therefore, although CPVT would require chronic administration, patients resistant to all other therapies may find benefits that outweigh ruxolitinib′s on-target effects.

CaMKAR′s high sensitivity and fast kinetics will enable elucidation of pathologic CaMKII activity dynamics with high spatiotemporal resolution. Furthermore, CaMKAR can be scaled in cell culture, which will permit more ambitious chemical screens. The molecules identified here can also serve as scaffolds for medicinal chemistry to amplify their CaMKII potency and minimize their originally intended effects. Given the lengthy regulatory approval process for novel compounds, it may be worth exploring potential cardiac indications for ruxolitinib itself. Last, although CaMKII is known to drive an extensive number of cardiac pathologies, it has been shown to underpin other illnesses, including asthma and cancer (*5*). Future study will be needed to determine the utility of our identified compounds in these diseases.

MATERIALS AND METHODS

Study design

The goal of this study was to engineer a CaMKII reporter suitable for high-throughput screening and identify drugs that can be repurposed as CaMKII inhibitors for cardiac indications. All animal studies were approved by appropriate animal care and use committees. Mice of both sexes were used unless noted in the methods. Animal number was determined by prior experience and published reports. Mice were randomly assigned to treatment conditions, and when an experiment spanned across multiple days, all conditions were represented in each cohort. Behavioral tests were performed by an independent experimenter blinded to the conditions. Experiments determining protection of ruxolitinib in CPVT models (cells and mice) were performed by experimenters blinded to the identity of the compound. Imaging data analysis was done in a computer-automated fashion to avoid human bias.

Statistics

Imaging summary data were condensed and organized with R Studio. Statistical testing was done with GraphPad Prism v8.2.0 as described in each figure. Normality was tested via Shapiro-Wilk with 0.05 alpha level. Signal-to-noise ratio was calculated as described (*37*): single-cell maximal ratio change after stimulation divided by the SD across four baseline time points.

Supplementary Materials

This PDF file includes:
Methods
Figs. S1 to S12
Tables S1 to S3
References (*92*–*118*)

Other Supplementary Material for this manuscript includes the following:
Data files S1 to S3
MDAR Reproducibility Checklist

View/request a protocol for this paper from *Bio-protocol*.

REFERENCES AND NOTES

1. G. A. Roth, G. A. Mensah, C. O. Johnson, G. Addolorato, E. Ammirati, L. M. Baddour, N. C. Barengo, A. Z. Beaton, E. J. Benjamin, C. P. Benziger, A. Bonny, M. Brauer, M. Brodmann, T. J. Cahill, J. Carapetis, A. L. Catapano, S. S. Chugh, L. T. Cooper, J. Coresh, M. Criqui, N. DeCleene, K. A. Eagle, S. Emmons-Bell, V. L. Feigin, J. Fernández-Solà, G. Fowkes, E. Gakidou, S. M. Grundy, F. J. He, G. Howard, F. Hu, L. Inker, G. Karthikeyan, N. Kassebaum, W. Koroshetz, C. Lavie, D. Lloyd-Jones, H. S. Lu, A. Mirijello, A. M. Temesgen, A. Mokdad, A. E. Moran, P. Muntner, J. Narula, B. Neal, M. Ntsekhe, G. Moraes de Oliveira, C. Otto, M. Owolabi, M. Pratt, S. Rajagopalan, M. Reitsma, A. L. P. Ribeiro, N. Rigotti, A. Rodgers, C. Sable, S. Shakil, K. Sliwa-Hahnle, B. Stark, J. Sundström, P. Timpel, I. M. Tleyjeh, M. Valgimigli, T. Vos, P. K. Whelton, M. Yacoub, L. Zuhlke, C. Murray, V. Fuster; GBD-NHLBI-JACC Global Burden of Cardiovascular Diseases Writing Group, Global burden of cardiovascular diseases and risk factors, 1990–2019: Update From the GBD 2019 Study. *J. Am. Coll. Cardiol.* **76**, 2982–3021 (2020).
2. Y. Wu, Z. Gao, B. Chen, O. M. Koval, M. V. Singh, X. Guan, T. J. Hund, W. Kutschke, S. Sarma, I. M. Grumbach, X. H. T. Wehrens, P. J. Mohler, L.-S. Song, M. E. Anderson, Calmodulin kinase II is required for fight or flight sinoatrial node physiology. *Proc. Natl. Acad. Sci. U.S.A.* **106**, 5972–5977 (2009).
3. M. M. Kreusser, L. H. Lehmann, S. Keranov, M.-O. Hoting, U. Oehl, M. Kohlhaas, J.-C. Reil, K. Neumann, M. D. Schneider, J. A. Hill, D. Dobrev, C. Maack, L. S. Maier, H.-J. Gröne, H. A. Katus, E. N. Olson, J. Backs, Cardiac CaM kinase II genes δ and γ contribute to adverse remodeling but redundantly inhibit calcineurin-induced myocardial hypertrophy. *Circulation* **130**, 1262–1273 (2014).
4. J. Beckendorf, M. M. G. van den Hoogenhof, J. Backs, Physiological and unappreciated roles of CaMKII in the heart. *Basic Res. Cardiol.* **113**, 29 (2018).
5. O. E. Reyes Gaido, L. J. Nkashama, K. L. Schole, Q. Wang, P. Umapathi, O. O. Mesubi, K. Konstantinidis, E. D. Luczak, M. E. Anderson, CaMKII as a therapeutic target in cardiovascular disease. *Annu. Rev. Pharmacol. Toxicol.* **63**, 249–272 (2023).
6. M. L. A. Joiner, O. M. Koval, J. Li, B. Julie He, C. Allamargot, Z. Gao, E. D. Luczak, D. D. Hall, B. D. Fink, B. Chen, J. Yang, S. A. Moore, T. D. Scholz, S. Strack, P. J. Mohler, W. I. Sivitz, L. S. Song, M. E. Anderson, CaMKII determines mitochondrial stress responses in heart. *Nature* **491**, 269–273 (2012).
7. R. Zhang, M. S. C. Khoo, Y. Wu, Y. Yang, C. E. Grueter, G. Ni, E. E. Price, W. Thiel, S. Guatimosim, L. S. Song, E. C. Madu, A. N. Shah, T. A. Vishnivetskaya, J. B. Atkinson, V. V. Gurevich, G. Salama, W. J. Lederer, R. J. Colbran, M. E. Anderson, Calmodulin kinase II inhibition protects against structural heart disease. *Nat. Med.* **11**, 409–417 (2005).
8. C. E. Grueter, R. J. Colbran, M. E. Anderson, CaMKII, an emerging molecular driver for calcium homeostasis, arrhythmias, and cardiac dysfunction. *J. Mol. Med.* **85**, 5–14 (2007).
9. B. J. He, M. L. A. Joiner, M. V. Singh, E. D. Luczak, P. D. Swaminathan, O. M. Koval, W. Kutschke, C. Allamargot, J. Yang, X. Guan, K. Zimmerman, I. M. Grumbach, R. M. Weiss, D. R. Spitz, C. D. Sigmund, W. M. Blankesteijn, S. Heymans, P. J. Mohler, M. E. Anderson, Oxidation of CaMKII determines the cardiotoxic effects of aldosterone. *Nat. Med.* **17**, 1610–1618 (2011).
10. E. Di Pasquale, F. Lodola, M. Miragoli, M. Denegri, J. E. Avelino-Cruz, M. Buonocore, H. Nakahama, P. Portararo, R. Bloise, C. Napolitano, G. Condorelli, S. G. Priori, CaMKII inhibition rectifies arrhythmic phenotype in a patient-specific model of catecholaminergic polymorphic ventricular tachycardia. *Cell Death Dis.* **4**, e843 (2013).
11. K. Konstantinidis, V. J. Bezzerides, L. Lai, H. M. Isbell, A. C. Wei, Y. Wu, M. C. Viswanathan, I. D. Blum, J. M. Granger, D. Heims-Waldron, D. Zhang, E. D. Luczak, K. R. Murphy, F. Lu, D. H. Gratz, B. Manta, Q. Wang, Q. Wang, A. L. Kolodkin, V. N. Gladyshev, T. J. Hund, W. T. Pu, M. N. Wu, A. Cammarato, M. A. Bianchet, M. A. Shea, R. L. Levine, M. E. Anderson, MICAL1 constrains cardiac stress responses and protects against disease by oxidizing CaMKII. *J. Clin. Invest.* **130**, 4663–4678 (2020).
12. Y. Wu, Q. Wang, N. Feng, J. M. Granger, M. E. Anderson, Myocardial death and dysfunction after ischemia-reperfusion injury require CaMKIIδ oxidation. *Sci. Rep.* **9**, 9291 (2019).
13. V. J. Bezzerides, A. Caballero, S. Wang, Y. Ai, R. J. Hylind, F. Lu, D. A. Heims-Waldron, K. D. Chambers, D. Zhang, D. J. Abrams, W. T. Pu, Gene therapy for catecholaminergic polymorphic ventricular tachycardia by inhibition of Ca^{2+}/calmodulin-dependent kinase II. *Circulation* **140**, 405–419 (2019).
14. M. Dewenter, S. Neef, C. Vettel, S. Lämmle, C. Beushausen, L. C. Zelarayan, S. Katz, A. von der Lieth, S. Meyer-Roxlau, S. Weber, T. Wieland, S. Sossalla, J. Backs, J. H. Brown, L. S. Maier,

A. El-Armouche, Calcium/calmodulin-dependent protein kinase II activity persists during chronic β-adrenoceptor blockade in experimental and human heart failure. *Circ. Heart Fail.* **10**, e003840 (2017).
15. H. Tokumitsu, T. Chijiwa, M. Hagiwara, A. Mizutani, M. Terasawa, H. Hidaka, KN-62, 1-[*N*,*O*-bis(5-isoquinolinesulfonyl)-*N*-methyl-L-tyrosyl]-4-phenylpiperazi ne, a specific inhibitor of Ca2+/calmodulin-dependent protein kinase II. *J. Biol. Chem.* **265**, 4315–4320 (1990).
16. M. Sumi, K. Kiuchi, T. Ishikawa, A. Ishii, M. Hagiwara, T. Nagatsu, H. Hidaka, The newly synthesized selective $Ca2^+$/calmodulin dependent protein kinase II inhibitor KN-93 reduces dopamine contents in PC12h cells. *Biochem. Biophys. Res. Commun.* **181**, 968–975 (1991).
17. M. Vila-Petroff, M. A. Salas, M. Said, C. A. Valverde, L. Sapia, E. Portiansky, R. J. Hajjar, E. G. Kranias, C. Mundiña-Weilenmann, A. Mattiazzi, CaMKII inhibition protects against necrosis and apoptosis in irreversible ischemia–reperfusion injury. *Cardiovasc. Res.* **73**, 689–698 (2007).
18. J. Ledoux, D. Chartier, N. Leblanc, Inhibitors of calmodulin-dependent protein kinase are nonspecific blockers of voltage-dependent K^+ channels in vascular myocytes. *J. Pharmacol. Exp. Ther.* **290**, 1165–1174 (1999).
19. S. Rezazadeh, T. W. Claydon, D. Fedida, KN-93 (2-[*N*-(2-hydroxyethyl)]-*N*-(4-methoxybenzenesulfonyl)amino-*N*-(4-chlorocinnamyl)-*N*-methylbenzylamine), a calcium/calmodulin-dependent protein kinase II inhibitor, is a direct extracellular blocker of voltage-gated potassium channels. *J. Pharmacol. Exp. Ther.* **317**, 292–299 (2006).
20. B. Hegyi, Y. Chen-Izu, Z. Jian, R. Shimkunas, L. T. Izu, T. Banyasz, KN-93 inhibits IKr in mammalian cardiomyocytes. *J. Mol. Cell. Cardiol.* **89**, 173–176 (2015).
21. M. H. Wong, A. B. Samal, M. Lee, J. Vlach, N. Novikov, A. Niedziela-Majka, J. Y. Feng, D. O. Koltun, K. M. Brendza, H. J. Kwon, B. E. Schultz, R. Sakowicz, J. S. Saad, G. A. Papalia, The KN-93 molecule inhibits calcium/calmodulin-dependent protein kinase II (CaMKII) activity by binding to Ca^{2+}/CaM. *J. Mol. Biol.* **431**, 1440–1459 (2019).
22. B. H. Chang, S. Mukherji, T. R. Soderling, Characterization of a calmodulin kinase II inhibitor protein in brain. *Proc. Natl. Acad. Sci. U.S.A.* **95**, 10890–10895 (1998).
23. R. S. Vest, K. D. Davies, H. O'Leary, J. D. Port, K. U. Bayer, Dual mechanism of a natural CaMKII inhibitor. *Mol. Biol. Cell* **18**, 5024–5033 (2007).
24. P. Pellicena, H. Schulman, CaMKII inhibitors: From research tools to therapeutic agents. *Front. Pharmacol.* **140**, 405–419 (2014).
25. S. Neef, A. Steffens, P. Pellicena, J. Mustroph, S. Lebek, K. R. Ort, H. Schulman, L. S. Maier, Improvement of cardiomyocyte function by a novel pyrimidine-based CaMKII-inhibitor. *J. Mol. Cell. Cardiol.* **115**, 73–81 (2018).
26. S. Lebek, A. Plößl, M. Baier, J. Mustroph, D. Tarnowski, C. M. Lücht, S. Schopka, B. Flörchinger, C. Schmid, Y. Zausig, N. Pagratis, B. Marchand, D. O. Koltun, W. K. Hung, S. Ahmadyar, L. Belardinelli, L. S. Maier, S. Wagner, The novel CaMKII inhibitor GS-680 reduces diastolic SR Ca leak and prevents CaMKII-dependent pro-arrhythmic activity. *J. Mol. Cell. Cardiol.* **118**, 159–168 (2018).
27. P. Beauverger, M.-L. Ozoux, G. Bégis, V. Glénat, V. Briand, M.-C. Philippo, C. Daveu, G. Tavares, S. Roy, A. Corbier, P. Briand, O. Dorchies, A.-L. Bauchet, E. Nicolai, O. Duclos, D. Tamarelle, M.-P. Pruniaux, A. J. Muslin, P. Janiak, Reversion of cardiac dysfunction by a novel orally available calcium/calmodulin-dependent protein kinase II inhibitor, RA306, in a genetic model of dilated cardiomyopathy. *Cardiovasc. Res.* **116**, 329–338 (2020).
28. J. Zhang, R. Liang, K. Wang, W. Zhang, M. Zhang, L. Jin, P. Xie, W. Zheng, H. Shang, Q. Hu, J. Li, G. Chen, F. Wu, F. Lan, L. Wang, S.-Q. Wang, Y. Li, Y. Zhang, J. Liu, F. Lv, X. Hu, R.-P. Xiao, X. Lei, Y. Zhang, Novel CaMKII-δ inhibitor hesperadin exerts dual functions to ameliorate cardiac ischemia/reperfusion injury and inhibit tumor growth. *Circulation* **145**, 1154–1168 (2022).
29. N. R. Lim, C. J. Thomas, L. S. Silva, Y. Y. Yeap, S. Yap, J. R. Bell, L. M. D. Delbridge, M. A. Bogoyevitch, O. L. Woodman, S. J. Williams, C. N. May, D. C. H. Ng, Cardioprotective 3′,4′-dihydroxyflavonol attenuation of JNK and p38MAPK signalling involves CaMKII inhibition. *Biochem. J.* **456**, 149–161 (2013).
30. A. J. Boyle, C. Schultz, J. B. Selvanayagam, S. Moir, R. Kovacs, N. Dib, D. Zlotnick, M. Al-Omary, S. Sugito, A. Selvarajah, N. Collins, G. McLachlan, Calcium/calmodulin-dependent protein kinase II delta inhibition and ventricular remodeling after myocardial infarction. *JAMA Cardiol.* **6**, 762–768 (2021).
31. M. E. Anderson, To be or not to be a CaMKII inhibitor? *JAMA Cardiol.* **6**, 769–770 (2021).
32. J. Lisman, R. Yasuda, S. Raghavachari, Mechanisms of CaMKII action in long-term potentiation. *Nat. Rev. Neurosci.* **13**, 169–182 (2012).
33. K. Takao, K.-I. Okamoto, T. Nakagawa, R. L. Neve, T. Nagai, A. Miyawaki, T. Hashikawa, S. Kobayashi, Y. Hayashi, Visualization of synaptic Ca^{2+} /calmodulin-dependent protein kinase II activity in living neurons. *J. Neurosci.* **25**, 3107–3112 (2005).
34. J. R. Erickson, R. Patel, A. Ferguson, J. Bossuyt, D. M. Bers, Fluorescence resonance energy transfer–based sensor Camui provides new insight into mechanisms of calcium/calmodulin-dependent protein kinase II activation in intact cardiomyocytes. *Circ. Res.* **109**, 729–738 (2011).
35. G. Ardestani, M. C. West, T. J. Maresca, R. A. Fissore, M. M. Stratton, FRET-based sensor for CaMKII activity (FRESCA): A useful tool for assessing CaMKII activity in response to Ca^{2+} oscillations in live cells. *J. Biol. Chem.* **294**, 11876–11891 (2019).
36. A. I. Kostyuk, A. D. Demidovich, D. A. Kotova, V. V. Belousov, D. S. Bilan, Circularly permuted fluorescent protein-based indicators: History, principles, and classification. *Int. J. Mol. Sci.* **20**, 4200 (2019).
37. S. Mehta, Y. Zhang, R. H. Roth, J. Zhang, A. Mo, B. Tenner, R. L. Huganir, J. Zhang, Single-fluorophore biosensors for sensitive and multiplexed detection of signalling activities. *Nat. Cell Biol.* **20**, 1215–1225 (2018).
38. J.-F. Zhang, B. Liu, I. Hong, A. Mo, R. H. Roth, B. Tenner, W. Lin, J. Z. Zhang, R. S. Molina, M. Drobizhev, T. E. Hughes, L. Tian, R. L. Huganir, S. Mehta, J. Zhang, An ultrasensitive biosensor for high-resolution kinase activity imaging in awake mice. *Nat. Chem. Biol.* **17**, 39–46 (2021).
39. D. E. Levy, H. Schulman, B. R. Paraselli, N. S. Kumar, B. Dabbugoddu, C. Balasubramanyam, *CaMKII inhibitors and uses thereof, U.S. Patent 20170247374-A1 (2017)*.
40. D. E. Levy, H. Schulman, B. R. Paraselli, N. S. Kumar, B. Dabbugoddu, C. Balasubramanyam, CaMKII inhibitors and uses thereof, U.S. Patent 20200385383-A1 (2020).
41. B. T. Bajar, E. S. Wang, A. J. Lam, B. B. Kim, C. L. Jacobs, E. S. Howe, M. W. Davidson, M. Z. Lin, J. Chu, Improving brightness and photostability of green and red fluorescent proteins for live cell imaging and FRET reporting. *Sci. Rep.* **6**, 20889 (2016).
42. N. Punwani, S. Yeleswaram, X. Chen, J. Bowman, M. Soloviev, W. Williams, Evaluation of the effect of ruxolitinib on cardiac repolarization: A thorough QT study. *Clin. Pharmacol. Drug Dev.* **3**, 207–214 (2014).
43. X. Zhao, X. Y. Sheng, C. D. Payne, X. Zhang, F. Wang, Y. M. Cui, Pharmacokinetics, safety, and tolerability of single- and multiple-dose once-daily baricitinib in healthy chinese subjects: A randomized placebo-controlled study. *Clin. Pharmacol. Drug Dev.* **9**, 952–960 (2020).
44. B. Zhong, O. Campagne, R. Salloum, T. Purzner, C. F. Stewart, LC-MS/MS method for quantitation of the CK2 inhibitor silmitasertib (CX-4945) in human plasma, CSF, and brain tissue, and application to a clinical pharmacokinetic study in children with brain tumors. *J. Chromatogr. B Analyt. Technol. Biomed. Life Sci.* **1152**, 122254 (2020).
45. J. C. Panetta, S. D. Baker, H. M. Kantarjian, C. Stewart, B. Pond, M. Macaraeg, T. Makinde, S. Vali, N. Daver, A. Ramachandran, R. Collins, J. E. Cortes, Population pharmacokinetics of crenolanib, a type I FLT3 inhibitor, in patients with relapsed/refractory AML. *Blood* **126**, 3695 (2015).
46. A. Patnaik, L. S. Rosen, S. M. Tolaney, A. W. Tolcher, J. W. Goldman, L. Gandhi, K. P. Papadopoulos, M. Beeram, D. W. Rasco, J. F. Hilton, A. Nasir, R. P. Beckmann, A. E. Schade, A. D. Fulford, T. S. Nguyen, R. Martinez, P. Kulanthaivel, L. Q. Li, M. Frenzel, D. M. Cronier, E. M. Chan, K. T. Flaherty, P. Y. Wen, G. I. Shapiro, Efficacy and safety of abemaciclib, an inhibitor of CDK4 and CDK6, for patients with breast cancer, non–small cell lung cancer, and other solid tumors. *Cancer Discov.* **6**, 740–753 (2016).
47. M. A. Movsesian, M. Nishikawa, R. S. Adelstein, Phosphorylation of phospholamban by calcium-activated, phospholipid-dependent protein kinase. Stimulation of cardiac sarcoplasmic reticulum calcium uptake. *J. Biol. Chem.* **259**, 8029–8032 (1984).
48. H. K. Simmerman, J. H. Collins, J. L. Theibert, A. D. Wegener, L. R. Jones, Sequence analysis of phospholamban. Identification of phosphorylation sites and two major structural domains. *J. Biol. Chem.* **261**, 13333–13341 (1986).
49. A. Mattiazzi, E. Kranias, The role of CaMKII regulation of phospholamban activity in heart disease. *Front. Pharmacol.* **5**, 5 (2014).
50. A. Quintás-Cardama, K. Vaddi, P. Liu, T. Manshouri, J. Li, P. A. Scherle, E. Caulder, X. Wen, Y. Li, P. Waeltz, M. Rupar, T. Burn, Y. Lo, J. Kelley, M. Covington, S. Shepard, J. D. Rodgers, P. Haley, H. Kantarjian, J. S. Fridman, S. Verstovsek, Preclinical characterization of the selective JAK1/2 inhibitor INCB018424: therapeutic implications for the treatment of myeloproliferative neoplasms. *Blood* **115**, 3109–3117 (2010).
51. P. M. Reeves, M. A. Abbaslou, F. R. W. Kools, K. Vutipongsatorn, X. Tong, C. Gavegano, R. F. Schinazi, M. C. Poznansky, Ruxolitinib sensitizes ovarian cancer to reduced dose Taxol, limits tumor growth and improves survival in immune competent mice. *Oncotarget* **8**, 94040–94053 (2017).
52. R. Das, P. Guan, L. Sprague, K. Verbist, P. Tedrick, Q. A. An, C. Cheng, M. Kurachi, R. Levine, E. J. Wherry, S. W. Canna, E. M. Behrens, K. E. Nichols, Janus kinase inhibition lessens inflammation and ameliorates disease in murine models of hemophagocytic lymphohistiocytosis. *Blood* **127**, 1666–1675 (2016).
53. N. Mollé, S. Krichevsky, P. Kermani, R. T. Silver, E. Ritchie, J. M. Scandura, Ruxolitinib can cause weight gain by blocking leptin signaling in the brain via JAK2/STAT3. *Blood* **135**, 1062–1066 (2020).
54. S. Albeituni, K. C. Verbist, P. E. Tedrick, H. Tillman, J. Picarsic, R. Bassett, K. E. Nichols, Mechanisms of action of ruxolitinib in murine models of hemophagocytic lymphohistiocytosis. *Blood* **134**, 147–159 (2019).

55. N. Liu, Y. Ruan, M. Denegri, T. Bachetti, Y. Li, B. Colombi, C. Napolitano, W. A. Coetzee, S. G. Priori, Calmodulin kinase II inhibition prevents arrhythmias in RyR2(R4496C$^{+/-}$) mice with catecholaminergic polymorphic ventricular tachycardia. *J. Mol. Cell. Cardiol.* **50**, 214–222 (2011).
56. P. J. Kannankeril, B. M. Mitchell, S. A. Goonasekera, M. G. Chelu, W. Zhang, S. Sood, D. L. Kearney, C. I. Danila, M. De Biasi, X. H. T. Wehrens, R. G. Pautler, D. M. Roden, G. E. Taffet, R. T. Dirksen, M. E. Anderson, S. L. Hamilton, Mice with the R176Q cardiac ryanodine receptor mutation exhibit catecholamine-induced ventricular tachycardia and cardiomyopathy. *Proc. Natl. Acad. Sci. U.S.A.* **103**, 12179–12184 (2006).
57. M. G. Chelu, S. Sarma, S. Sood, S. Wang, R. J. van Oort, D. G. Skapura, N. Li, M. Santonastasi, F. U. Müller, W. Schmitz, U. Schotten, M. E. Anderson, M. Valderrábano, D. Dobrev, X. H. T. Wehrens, Calmodulin kinase II-mediated sarcoplasmic reticulum Ca2+ leak promotes atrial fibrillation in mice. *J. Clin. Invest.* **119**, 1940–1951 (2009).
58. A. Purohit, A. G. Rokita, X. Guan, B. Chen, O. M. Koval, N. Voigt, S. Neef, T. Sowa, Z. Gao, E. D. Luczak, H. Stefansdottir, A. C. Behunin, N. Li, R. N. El-Accaoui, B. Yang, P. D. Swaminathan, R. M. Weiss, X. H. T. Wehrens, L.-S. Song, D. Dobrev, L. S. Maier, M. E. Anderson, Oxidized Ca^{2+}/calmodulin-dependent protein kinase II triggers atrial fibrillation. *Circulation* **128**, 1748–1757 (2013).
59. O. O. Mesubi, A. G. Rokita, N. Abrol, Y. Wu, B. Chen, Q. Wang, J. M. Granger, A. Tucker-Bartley, E. D. Luczak, K. R. Murphy, P. Umapathi, P. S. Banerjee, T. N. Boronina, R. N. Cole, L. S. Maier, X. H. Wehrens, J. L. Pomerantz, L.-S. Song, R. S. Ahima, G. W. Hart, N. E. Zachara, M. E. Anderson, Oxidized CaMKII and *O*-GlcNAcylation cause increased atrial fibrillation in diabetic mice by distinct mechanisms. *J. Clin. Invest.* **131**, e95747 (2021).
60. W. B. Kannel, R. D. Abbott, D. D. Savage, P. M. McNamara, Epidemiologic features of chronic atrial fibrillation: The Framingham study. *N. Engl. J. Med.* **306**, 1018–1022 (1982).
61. J. R. Erickson, L. Pereira, L. Wang, G. Han, A. Ferguson, K. Dao, R. J. Copeland, F. Despa, G. W. Hart, C. M. Ripplinger, D. M. Bers, Diabetic hyperglycaemia activates CaMKII and arrhythmias by O-linked glycosylation. *Nature* **502**, 372–376 (2013).
62. P. Umapathi, P. S. Banerjee, N. E. Zachara, N. Abrol, Q. Wang, O. O. Mesubi, E. D. Luczak, Y. Wu, J. M. Granger, A.-C. Wei, O. E. Reyes Gaido, L. Florea, C. C. Talbot Jr., G. W. Hart, M. E. Anderson, Excessive *O*-GlcNAcylation causes heart failure and sudden death. *Circulation* **143**, 1687–1703 (2021).
63. F. U. Müller, G. Lewin, H. A. Baba, P. Bokník, L. Fabritz, U. Kirchhefer, P. Kirchhof, K. Loser, M. Matus, J. Neumann, B. Riemann, W. Schmitz, Heart-directed expression of a human cardiac isoform of cAMP-response element modulator in transgenic mice. *J. Biol. Chem.* **280**, 6906–6914 (2005).
64. N. Li, D. Y. Chiang, S. Wang, Q. Wang, L. Sun, N. Voigt, J. L. Respress, S. Ather, D. G. Skapura, V. K. Jordan, F. T. Horrigan, W. Schmitz, F. U. Müller, M. Valderrabano, S. Nattel, D. Dobrev, X. H. T. Wehrens, Ryanodine-receptor mediated calcium leak drives progressive development of an atrial fibrillation substrate in a transgenic mouse model. *Circulation* **129**, 1276–1285 (2014).
65. K. U. Bayer, H. Schulman, CaM kinase: Still inspiring at 40. *Neuron* **103**, 380–394 (2019).
66. Q. Zhang, Y. Zhang, S. Diamond, J. Boer, J. J. Harris, Y. Li, M. Rupar, E. Behshad, C. Gardiner, P. Collier, P. Liu, T. Burn, R. Wynn, G. Hollis, S. Yeleswaram, The Janus kinase 2 inhibitor fedratinib inhibits thiamine uptake: A putative mechanism for the onset of Wernicke's encephalopathy. *Drug Metab. Dispos.* **42**, 1656–1662 (2014).
67. G. L. Plosker, Ruxolitinib: A review of its use in patients with myelofibrosis. *Drugs* **75**, 297–308 (2015).
68. H. Wang, R. Feng, L. P. Wang, F. Li, X. Cao, J. Z. Tsien, CaMKII activation state underlies synaptic labile phase of LTP and short-term memory formation. *Curr. Biol.* **18**, 1546–1554 (2008).
69. M. E. Bach, R. D. Hawkins, M. Osman, E. R. Kandel, M. Mayford, Impairment of spatial but not contextual memory in CaMKII mutant mice with a selective loss of hippocampal LTP in the range of the θ frequency. *Cell* **81**, 905–915 (1995).
70. G. Zalcman, N. Federman, A. Romano, CaMKII isoforms in learning and memory: Localization and function. *Front. Mol. Neurosci.* **11**, 445 (2018).
71. H. Wang, E. Shimizu, Y.-P. Tang, M. Cho, M. Kyin, W. Zuo, D. A. Robinson, P. J. Alaimo, C. Zhang, H. Morimoto, M. Zhuo, R. Feng, K. M. Shokat, J. Z. Tsien, Inducible protein knockout reveals temporal requirement of CaMKII reactivation for memory consolidation in the brain. *Proc. Natl. Acad. Sci. U.S.A.* **100**, 4287–4292 (2003).
72. S. Moriguchi, H. Tagashira, Y. Sasaki, J. Z. Yeh, H. Sakagami, T. Narahashi, K. Fukunaga, CaMKII activity is essential for improvement of memory-related behaviors by chronic rivastigmine treatment. *J. Neurochem.* **128**, 927–937 (2014).
73. A. D. Bachstetter, S. J. Webster, T. Tu, D. S. Goulding, J. Haiech, D. M. Watterson, L. J. Van Eldik, Generation and behavior characterization of CaMKIIβ knockout mice. *PLOS ONE* **9**, e105191 (2014).
74. N. Federman, V. de la Fuente, G. Zalcman, N. Corbi, A. Onori, C. Passananti, A. Romano, Nuclear factor κB-dependent histone acetylation is specifically involved in persistent forms of memory. *J. Neurosci.* **33**, 7603–7614 (2013).
75. A. B. Nair, S. Jacob, A simple practice guide for dose conversion between animals and human. *J. Basic Clin. Pharm.* **7**, 27–31 (2016).
76. S. Verstovsek, H. Kantarjian, R. A. Mesa, A. D. Pardanani, J. Cortes-Franco, D. A. Thomas, Z. Estrov, J. S. Fridman, E. C. Bradley, S. Erickson-Viitanen, K. Vaddi, R. Levy, A. Tefferi, Safety and efficacy of INCB018424, a JAK1 and JAK2 inhibitor, in myelofibrosis. *N. Engl. J. Med.* **363**, 1117–1127 (2010).
77. A. D. Shilling, F. M. Nedza, T. Emm, S. Diamond, E. McKeever, N. Punwani, W. Williams, A. Arvanitis, L. G. Galya, M. Li, S. Shepard, J. Rodgers, T.-Y. Yue, S. Yeleswaram, Metabolism, excretion, and pharmacokinetics of [14C]INCB018424, a selective Janus tyrosine kinase 1/2 inhibitor, in humans. *Drug Metab. Dispos.* **38**, 2023–2031 (2010).
78. W. B. Haile, C. Gavegnano, S. Tao, Y. Jiang, R. F. Schinazi, W. R. Tyor, The Janus kinase inhibitor ruxolitinib reduces HIV replication in human macrophages and ameliorates HIV encephalitis in a murine model. *Neurobiol. Dis.* **92**, 137–143 (2016).
79. R. J. van Oort, M. D. McCauley, S. S. Dixit, L. Pereira, Y. Yang, J. L. Respress, Q. Wang, A. C. De Almeida, D. G. Skapura, M. E. Anderson, D. M. Bers, X. H. T. Wehrens, Ryanodine receptor phosphorylation by calcium/calmodulin-dependent protein kinase II promotes life-threatening ventricular arrhythmias in mice with heart failure. *Circulation* **122**, 2669–2679 (2010).
80. X. Pan, L. Philippen, S. K. Lahiri, C. Lee, S. H. Park, T. A. Word, N. Li, K. E. Jarrett, R. Gupta, J. O. Reynolds, J. Lin, G. Bao, W. R. Lagor, X. H. T. Wehrens, In vivo *Ryr* 2 editing corrects catecholaminergic polymorphic ventricular tachycardia. *Circ. Res.* **123**, 953–963 (2018).
81. S.-J. Park, D. Zhang, Y. Qi, Y. Li, K. Y. Lee, V. J. Bezzerides, P. Yang, S. Xia, S. L. Kim, X. Liu, F. Lu, F. S. Pasqualini, P. H. Campbell, J. Geva, A. E. Roberts, A. G. Kleber, D. J. Abrams, W. T. Pu, K. K. Parker, Insights into the pathogenesis of catecholaminergic polymorphic ventricular tachycardia from engineered human heart tissue. *Circulation* **140**, 390–404 (2019).
82. H. K. Al-Ali, M. Griesshammer, L. Foltz, G. A. Palumbo, B. Martino, F. Palandri, A. M. Liberati, P. le Coutre, C. García-Hernández, A. Zaritskey, R. Tavares, V. Gupta, P. Raanani, P. Giraldo, M. Hänel, D. Damiani, T. Sacha, C. Bouard, C. Paley, R. Tiwari, F. Mannelli, A. M. Vannucchi, Primary analysis of JUMP, a phase 3b, expanded-access study evaluating the safety and efficacy of ruxolitinib in patients with myelofibrosis, including those with low platelet counts. *Br. J. Haematol.* **189**, 888–903 (2020).
83. S. Verstovsek, R. A. Mesa, J. Gotlib, V. Gupta, J. F. DiPersio, J. V. Catalano, M. W. N. Deininger, C. B. Miller, R. T. Silver, M. Talpaz, E. F. Winton, J. H. Harvey, M. O. Arcasoy, E. O. Hexner, R. M. Lyons, R. Paquette, A. Raza, M. Jones, D. Kornacki, K. Sun, H. Kantarjian; COMFORT-I investigators, Long-term treatment with ruxolitinib for patients with myelofibrosis: 5-year update from the randomized, double-blind, placebo-controlled, phase 3 COMFORT-I trial. *J. Hematol. Oncol.* **10**, 55 (2017).
84. J. G. Shi, X. Chen, R. F. McGee, R. R. Landman, T. Emm, Y. Lo, P. A. Scherle, N. G. Punwani, W. V. Williams, S. Yeleswaram, The pharmacokinetics, pharmacodynamics, and safety of orally dosed INCB018424 phosphate in healthy volunteers. *J. Clin. Pharmacol.* **51**, 1644–1654 (2011).
85. D. Dobrev, M. Aguilar, J. Heijman, J.-B. Guichard, S. Nattel, Postoperative atrial fibrillation: Mechanisms, manifestations and management. *Nat. Rev. Cardiol.* **16**, 417–436 (2019).
86. J. P. Mathew, M. L. Fontes, I. C. Tudor, J. Ramsay, P. Duke, C. D. Mazer, P. G. Barash, P. H. Hsu, D. T. Mangano; for the Investigators of the Ischemia Research and Education Foundation; Multicenter Study of Perioperative Ischemia Research Group, A multicenter risk index for atrial fibrillation after cardiac surgery. *JAMA* **291**, 1720–1729 (2004).
87. R. H. Mehta, A. Z. Starr, R. D. Lopes, J. S. Hochman, P. Widimsky, K. S. Pieper, P. W. Armstrong, C. B. Granger; for the APEX AMI Investigators, Incidence of and outcomes associated with ventricular tachycardia or fibrillation in patients undergoing primary percutaneous coronary intervention. *JAMA* **301**, 1779–1789 (2009).
88. J. Heijman, A. P. Muna, T. Veleva, C. E. Molina, H. Sutanto, M. Tekook, Q. Wang, I. H. Abu-Taha, M. Gorka, S. Künzel, A. El-Armouche, H. Reichenspurner, M. Kamler, V. Nikolaev, U. Ravens, N. Li, S. Nattel, X. H. T. Wehrens, D. Dobrev, Atrial myocyte NLRP3/CaMKII nexus forms a substrate for postoperative atrial fibrillation. *Circ. Res.* **127**, 1036–1055 (2020).
89. J. R. Bell, M. Vila-Petroff, L. M. D. Delbridge, CaMKII-dependent responses to ischemia and reperfusion challenges in the heart. *Front. Pharmacol.* **5**, 96 (2014).
90. Y. Tsuji, M. Hojo, N. Voigt, A. El-Armouche, Y. Inden, T. Murohara, D. Dobrev, S. Nattel, I. Kodama, K. Kamiya, Ca^{2+}-related signaling and protein phosphorylation abnormalities play central roles in a new experimental model of electrical storm. *Circulation* **123**, 2192–2203 (2011).
91. T. M. Roston, K. Jones, N. M. Hawkins, J. M. Bos, P. J. Schwartz, F. Perry, M. J. Ackerman, Z. W. M. Laksman, P. Kaul, K. V. V. Lieve, J. Atallah, A. D. Krahn, S. Sanatani, Implantable cardioverter-defibrillator use in catecholaminergic polymorphic ventricular tachycardia: A systematic review. *Heart Rhythm* **15**, 1791–1799 (2018).
92. S. Mishra, N. Sadagopan, B. Dunkerly-Eyring, S. Rodriguez, D. C. Sarver, R. P. Ceddia, S. A. Murphy, H. Knutsdottir, V. P. Jani, D. Ashok, C. U. Oeing, B. O'Rourke, J. A. Gangoiti, D. D. Sears, G. W. Wong, S. Collins, D. A. Kass, Inhibition of phosphodiesterase type 9 reduces obesity and cardiometabolic syndrome in mice. *J. Clin. Invest.* **131**, e148798 (2021).

93. N. Pavlaki, K. A. De Jong, B. Geertz, V. O. Nikolaev, A. Froese, Cardiac hypertrophy changes compartmentation of cAMP in non-raft membrane microdomains. *Cell* **10**, 535 (2021).
94. S. Eid, S. Turk, A. Volkamer, F. Rippmann, S. Fulle, KinMap: A web-based tool for interactive navigation through human kinome data. *BMC Bioinformatics* **18**, 16 (2017).
95. P. C. Taylor, T. Takeuchi, G. R. Burmester, P. Durez, J. S. Smolen, W. Deberdt, M. Issa, J. R. Terres, N. Bello, K. L. Winthrop, Safety of baricitinib for the treatment of rheumatoid arthritis over a median of 4.6 and up to 9.3 years of treatment: Final results from long-term extension study and integrated database. *Ann. Rheum. Dis.* **81**, 335–343 (2022).
96. H. S. Rugo, J. Huober, J. A. García-Sáenz, N. Masuda, J. H. Sohn, V. A. M. Andre, S. Barriga, J. Cox, M. Goetz, Management of abemaciclib-associated adverse events in patients with hormone receptor-positive, human epidermal growth factor receptor 2-negative advanced breast cancer: Safety analysis of MONARCH 2 and MONARCH 3. *Oncologist* **26**, e53–e65 (2021).
97. S. Johnston, M. Martin, A. Di Leo, S.-A. Im, A. Awada, T. Forrester, M. Frenzel, M. C. Hardebeck, J. Cox, S. Barriga, M. Toi, H. Iwata, M. P. Goetz, MONARCH 3 final PFS: a randomized study of abemaciclib as initial therapy for advanced breast cancer. *Npj Breast Cancer* **5**, 5 (2019).
98. M. J. Borad, L.-Y. Bai, M.-H. Chen, J. M. Hubbard, K. Mody, S. Y. Rha, D. A. Richards, S. L. Davis, J. Soong, C.-E. C.-E. Huang, E. Tse, D. H. Ahn, H.-M. Chang, C.-J. Yen, D.-Y. Oh, J. O. Park, C. Hsu, C. R. Becerra, J.-S. Chen, Y.-Y. Chen, Silmitasertib (CX-4945) in combination with gemcitabine and cisplatin as first-line treatment for patients with locally advanced or metastatic cholangiocarcinoma: A phase Ib/II study. *J. Clin. Oncol.* **39**, 312–312 (2021).
99. E. S. Wang, A. D. Goldberg, R. B. Walter, R. Collins, R. M. Stone, Long-term results of a phase 2 trial of crenolanib combined with 7+3 chemotherapy in adults with newly diagnosed FLT3 mutant AML. *J. Clin. Oncol.* **40**, 7007–7007 (2022).
100. M. Wu, C. Li, X. Zhu, FLT3 inhibitors in acute myeloid leukemia. *J. Hematol. Oncol.* **11**, 133 (2018).
101. Incyte Corporation, JAKAFI (ruxolitinib) tablets, for oral use [package insert]; www.accessdata.fda.gov/drugsatfda_docs/label/2021/202192s023lbl.pdf.
102. Eli Lilly and Company, OLUMIANT (baricitinib) tablets, for oral use; www.accessdata.fda.gov/drugsatfda_docs/label/2022/207924s006lbl.pdf.
103. S. C. J. Jorgensen, C. L. Y. Tse, L. Burry, L. D. Dresser, Baricitinib: A review of pharmacology, safety, and emerging clinical experience in COVID-19. *Pharmacotherapy* **40**, 843–856 (2020).
104. Eli Lilly and Company, VERZENIO (abemaciclib) tablets, for oral use; www.accessdata.fda.gov/drugsatfda_docs/label/2021/208716s006s007s008lbl.pdf.
105. A. Galanis, H. Ma, T. Rajkhowa, A. Ramachandran, D. Small, J. Cortes, M. Levis, Crenolanib is a potent inhibitor of FLT3 with activity against resistance-conferring point mutants. *Blood* **123**, 94–100 (2014).
106. S. R. D. Johnston, N. Harbeck, R. Hegg, M. Toi, M. Martin, Z. M. Shao, Q. Y. Zhang, J. L. Martinez Rodriguez, M. Campone, E. Hamilton, J. Sohn, V. Guarneri, M. Okada, F. Boyle, P. Neven, J. Cortés, J. Huober, A. Wardley, S. M. Tolaney, I. Cicin, I. C. Smith, M. Frenzel, D. Headley, R. Wei, B. San Antonio, M. Hulstijn, J. Cox, J. O'Shaughnessy, P. Rastogi; on behalf of the monarchE Committee Members and Investigators, Abemaciclib combined with endocrine therapy for the adjuvant treatment of HR^{+}, $HER2^{-}$, node-positive, high-risk, early breast cancer (monarchE). *J. Clin. Oncol.* **38**, 3987–3998 (2020).
107. J. K. Randhawa, H. M. Kantarjian, G. Borthakur, P. A. Thompson, M. Konopleva, N. Daver, N. Pemmaraju, E. Jabbour, T. M. Kadia, Z. Estrov, A. Ramachandran, J. Paradela, M. Andreef, M. Levis, F. Ravandi, J. E. Cortes, Results of a phase II study of crenolanib in relapsed/refractory acute myeloid leukemia patients (Pts) with activating FLT3 mutations. *Blood* **124**, 389 (2014).
108. C. Gavegnano, W. B. Haile, S. Hurwitz, S. Tao, Y. Jiang, R. F. Schinazi, W. R. Tyor, Baricitinib reverses HIV-associated neurocognitive disorders in a SCID mouse model and reservoir seeding in vitro. *J. Neuroinflammation* **16**, 182 (2019).
109. T. J. Raub, G. N. Wishart, P. Kulanthaivel, B. A. Staton, R. T. Ajamie, G. A. Sawada, L. M. Gelbert, H. E. Shannon, C. Sanchez-Martinez, A. D. Dios, Brain exposure of two selective dual CDK4 and CDK6 inhibitors and the antitumor activity of CDK4 and CDK6 inhibition in combination with temozolomide in an intracranial glioblastoma xenograft. *Drug Metab. Dispos.* **43**, 1360–1371 (2015).
110. J. S. Fridman, P. A. Scherle, R. Collins, T. C. Burn, Y. Li, J. Li, M. B. Covington, B. Thomas, P. Collier, M. F. Favata, X. Wen, J. Shi, R. McGee, P. J. Haley, S. Shepard, J. D. Rodgers, S. Yeleswaram, G. Hollis, R. C. Newton, B. Metcalf, S. M. Friedman, K. Vaddi, Selective inhibition of JAK1 and JAK2 is efficacious in rodent models of arthritis: Preclinical characterization of INCB028050. *J. Immunol.* **184**, 5298–5307 (2010).
111. J. Jiang, K. Ghoreschi, F. Deflorian, Z. Chen, M. Perreira, M. Pesu, J. Smith, D.-T. Nguyen, E. H. Liu, W. Leister, S. Costanzi, J. J. O'Shea, C. J. Thomas, Examining the chirality, conformation and selective kinase inhibition of 3-((3*R*,4*R*)-4-methyl-3-(methyl(7*H*-pyrrolo[2,3-*d*]pyrimidin-4-yl)amino)piperidin-1-yl)-3-oxopropanenitrile (CP-690,550). *J. Med. Chem.* **51**, 8012–8018 (2008).
112. M. Ito, S. Yamazaki, K. Yamagami, M. Kuno, Y. Morita, K. Okuma, K. Nakamura, N. Chida, M. Inami, T. Inoue, S. Shirakami, Y. Higashi, A novel JAK inhibitor, peficitinib, demonstrates potent efficacy in a rat adjuvant-induced arthritis model. *J. Pharmacol. Sci.* **133**, 25–33 (2017).
113. G. Wernig, M. G. Kharas, R. Okabe, S. A. Moore, D. S. Leeman, D. E. Cullen, M. Gozo, E. P. McDowell, R. L. Levine, J. Doukas, C. C. Mak, G. Noronha, M. Martin, Y. D. Ko, B. H. Lee, R. M. Soll, A. Tefferi, J. D. Hood, D. G. Gilliland, Efficacy of TG101348, a selective JAK2 inhibitor, in treatment of a murine model of JAK2V617F-induced polycythemia vera. *Cancer Cell* **13**, 311–320 (2008).
114. L. Van Rompaey, R. Galien, E. M. van der Aar, P. Clement-Lacroix, L. Nelles, B. Smets, L. Lepescheux, T. Christophe, K. Conrath, N. Vandeghinste, B. Vayssiere, S. De Vos, S. Fletcher, R. Brys, G. tvan ' Klooster, J. H. M. Feyen, C. Menet, Preclinical characterization of GLPG0634, a selective inhibitor of JAK1, for the treatment of inflammatory diseases. *J. Immunol.* **191**, 3568–3577 (2013).
115. G. Coffey, A. Betz, F. DeGuzman, Y. Pak, M. Inagaki, D. C. Baker, S. J. Hollenbach, A. Pandey, U. Sinha, The novel kinase inhibitor PRT062070 (cerdulatinib) demonstrates efficacy in models of autoimmunity and B-cell cancer. *J. Pharmacol. Exp. Ther.* **351**, 538–548 (2014).
116. L. Ma, J. R. Clayton, R. A. Walgren, B. Zhao, R. J. Evans, M. C. Smith, K. M. Heinz-Taheny, E. L. Kreklau, L. Bloem, C. Pitou, W. Shen, J. M. Strelow, C. Halstead, M. E. Rempala, S. Parthasarathy, J. R. Gillig, L. J. Heinz, H. Pei, Y. Wang, L. F. Stancato, M. S. Dowless, P. W. Iversen, T. P. Burkholder, Discovery and characterization of LY2784544, a small-molecule tyrosine kinase inhibitor of JAK2V617F. *Blood Cancer J.* **3**, e109 (2013).
117. A. Pardanani, T. Lasho, G. Smith, C. J. Burns, E. Fantino, A. Tefferi, CYT387, a selective JAK1/JAK2 inhibitor: In vitro assessment of kinase selectivity and preclinical studies using cell lines and primary cells from polycythemia vera patients. *Leukemia* **23**, 1441–1445 (2009).
118. A. J. Gonzales, J. W. Bowman, G. J. Fici, M. Zhang, D. W. Mann, M. Mitton-Fry, Oclacitinib (APOQUEL) is a novel Janus kinase inhibitor with activity against cytokines involved in allergy. *J. Vet. Pharmacol. Ther.* **37**, 317–324 (2014).

Acknowledgments: We are thankful to the Johns Hopkins Biostatistics, Epidemiology, and Data Management (BEAD) Core for statistical analysis stewardship, Fondation Leducq for providing the AS100397 compound, D. A. Kass and F. Wu for providing NRVMs, and J. Yang for animal maintenance. **Funding:** These studies were supported by the American Heart Association Predoctoral Fellowship 905878 (to O.E.R.G.); NIH grants R35HL140034 (to M.E.A.), K08HL140197 (to V.J.B.), K12HL141952 (to O.O.M.), UG3TR003279-02 (to D.W.), R01HL089598, R01HL147108, R01HL153350, R01HL160992 (to X.H.T.W.), RF1MH126707 (to R.L.H.), and K99HL155840 (to B.L.L.); the Sarnoff Fellowship (to L.J.N.); the Translational Research Program at Boston Children's Hospital (to N.P.); the RWJF/AHA Harold Amos Faculty Development Program Grant 967117 (to O.O.M.); and the Flight Attendant Medical Research Institute (to J.O.L.). **Author contributions:** O.E.R.G. and M.E.A. conceptualized the study. O.E.R.G., N.P., and V.J.B. created the original draft of the manuscript. O.E.R.G., N.P., M.E.A., and V.J.B. reviewed and edited the final manuscript. O.E.R.G., N.P., A.L., B.L.L., F.U.M., R.L.H., X.H.T.W., and J.O.L. developed the methodology. O.E.R.G., N.P., J.M.G., L.J.N., D.W., J.M., C.E.T., O.O.M., K.L.S., B.L., M.M.H., L.E.D., K.M.F., E.D.L., and V.J.B. carried out the experimental studies. O.E.R.G. and N.P. created visual representations of the data. **Competing interests:** O.E.R.G., E.D.L., and M.E.A. are authors on two provisional patents [Inhibitors of calcium/calmodulin-dependent protein kinase II and their uses (#63/390,789) and Biosensor and uses thereof (#63/323,968)] derived from this work. O.O.M. is a paid consultant for Broadview Ventures Inc. All other authors declare that they have no competing interests. **Data and materials availability:** All data associated with this study are present in the paper or the Supplementary Materials. CREM-IbΔC-X–overexpressing mice are available from X.H.T.W. and F.U.M. through a material transfer agreement with the University of Münster. Raw image files, CaMKAR plasmids, and the AS100397 compound are available through a material transfer agreement upon request (contact E.D.L. at betsy.luczak@jhmi.edu).

Submitted 12 October 2022
Resubmitted 06 March 2023
Accepted 31 May 2023
Published 21 June 2023
10.1126/scitranslmed.abq7839